On the "screamer-like" birds from the British London Clay: An archaic anseriform-galliform mosaic and a non-galloanserine "barb-necked" species of *Perplexicervix*

Gerald Mayr, Vicen Carrió, and Andrew C. Kitchener

ABSTRACT

We revisit recently described putative anseriform birds from the early Eocene London Clay of Walton-on-the-Naze (Essex, UK). Phylogenetically relevant skeletal elements of *Danielsavis nazensis* Houde et al., 2023 are reported that were omitted from the original description, including the pterygoids and palatines. We detail that anseriform affinities of *D. nazensis* are not strongly supported and that the species shares presumably derived characteristics with the Galliformes. Actually, it is not straightforward to determine whether *Danielsavis* is a galliform-like stem group anseriform or whether it represents an anseriform-like stem group galliform, and our re-analysis of an emended data matrix from the original description supported galliform affinities. If *D. nazensis* is an anseriform bird, it is the phylogenetically earliest-diverging currently known, and in view of its morphological distinctness, the species is here assigned to a new taxon (Danielsavidae, fam. nov.). Among the material that was previously likened to *Danielsavis* are various fossils, which are not from galloanserine birds. Some of these have cervical vertebrae with an unusual tuberculate surface and are assigned to *Perplexicervix* Mayr, 2010, within the new taxon Perplexicervicidae, fam. nov. A new species, *P. paucituberculata*, is described and postcranial elements that are tentatively referred to this species show a resemblance to the Otidiformes (bustards). If a classification into the Otidiformes is corroborated by future studies, the fossils would constitute the first formally described Paleogene record of this Old World group of birds.

Gerald Mayr. Ornithological Section, Senckenberg Research Institute and Natural History Museum Frankfurt, Senckenberganlage 25, 60325 Frankfurt am Main, Germany, *Corresponding author Gerald.Mayr@senckenberg.de
Vicen Carrió. Department of Natural Sciences, National Museums Scotland, Chambers Street, Edinburgh

EH1 1JF, UK. v.carrio@nms.ac.uk
Andrew C. Kitchener. Department of Natural Sciences, National Museums Scotland, Chambers Street, Edinburgh EH1 1JF, UK and School of Geosciences, University of Edinburgh, Drummond Street, Edinburgh EH8 9XP, UK. a.kitchener@nms.ac.uk

---

INTRODUCTION

Galloanseres, the clade including Galliformes and Anseriformes, is the sister taxon of all other neognathous birds (Prum et al., 2015; Kuhl et al., 2021). The early Paleogene fossil record of stem group Galliformes is rather limited, and the known taxa exhibit morphologies similar to those of their extant relatives (Mayr, 2022). By contrast, the Paleocene and early Eocene record of anseriforms has much improved in recent years and includes morphologically diverse taxa, such as the Paleocene *Conflicto antarcticus* from Antarctica (Tambussi et al., 2019), the geographically and temporally widely distributed Presbyornithidae (Olson and Feduccia, 1980; Ericson, 2000; Kurochkin and Dyke, 2010; De Pietri et al., 2016; Zelenkov, 2021), as well as the early Eocene *Nettapterornis ("Anatalavis") oxfordi* from the London Clay of Walton-on-the-Naze (Essex, UK; Olson, 1999).

In a recent study, Houde et al. (2023) described a well-preserved partial skeleton of an anseriform bird from the late Paleocene of Wyoming (USA) as *Anachronornis anhimops*, within the new taxon Anachronornithidae. The authors also reported partial skeletons from Walton-on-the-Naze, which they considered to be "generally similar to but distinct from Anachronornithidae" (Houde et al., 2023: 25). One of these fossils was described as a new species, *Danielsavis nazensis*, and others went unnamed. As detailed further below, some of these latter specimens are neither morphologically close to *Danielsavis* nor do they belong to Galloanseres.

Among the unnamed species are specimens with vertebrae showing unusual tuberculate surfaces. These vertebrae were figured by Mayr (2022: figure 4.10e), who likened the fossils from the London Clay to *Perplexicervix microcephalon* from the latest early or earliest middle Eocene of the Messel fossil site in Germany; possible affinities to *Perplexicervix* were also considered by Houde et al. (2023). *Perplexicervix microcephalon* is known from several skeletons and is character-ised by the occurrence of numerous small barb-like tubercles on the surfaces of the cervical vertebrae (Mayr, 2007, 2010). Mayr (2007) hypothesised that these structures may be of pathological origin, but their subsequent recognition in multiple specimens of the same species (Mayr, 2010) challenges this assumption.

The London Clay fossils were compared to the Anhimidae by Mayr (2022: 60, figure 4.10), who mentioned some similarities and differences, but only briefly examined the specimens during a visit to the Daniels collection in 2008. Houde et al. (2023) described the major bones of *Danielsavis nazensis*, but did not comment on various phylogenetically relevant skeletal elements preserved in the fossils. Here, we provide an emended description of the *D. nazensis* fossils and detail that anseriform affinities of the species are only weakly supported. Furthermore, we show that the *Perplexicervix*–like fossils that were likened to *Danielsavis* by Houde et al. (2023) are not from a representative of the Galloanseres, but belong to a neoavian species, which shows a resemblance to the Otidiformes (bustards).

MATERIAL AND METHODS

The fossils are deposited in the American Museum of Natural History, New York, USA (AMNH); the Hessisches Landesmuseum, Darmstadt, Germany (HLMD); the Royal Belgian Institute of Natural Sciences, Brussels, Belgium (IRSNB); the Natural History Museum, London, UK (NHMUK); the Naturhistorisches Museum Basel, Switzerland (NMB); the National Museums Scotland, Edinburgh, UK (NMS); the Senckenberg Research Institute Frankfurt, Germany (SMF); and the Wyoming Dinosaur Center, Thermopolis, USA (WDC).

In order to analyse the affinities of *Danielsavis*, we added new scorings and characters to the dataset 1 of Houde et al. (2023). For *Danielsavis*, scorings were added for four characters, which were coded as unknown by Houde et al. (2023): Ch. 4: d; ch. 6: d; ch. 128: b; ch. 129: a. Eight char-

acters were newly added to the matrix: Ch. 134: humerus, proximal end large with ratio humerus length to width of proximal end being less than 3.6: no (a); yes (b) – our scoring in the taxon sequence of Houde et al. (2023: supplementary data C) is aaaaabab *[Anachronornis, Anhimidae, Anseranas, Dendrocygna, Bucephala, Crax, Burhinus, Danielsavis];* ch. 135: humerus, tuberculum large and proximodistally long, with proximodistal length being greater than mediolateral width: no (a), yes (b) – scoring is aaaaabab; ch. 136: ulna, cotyla dorsalis reaching much farther distally than cotyla ventralis: no (a), yes (b) – scoring is aaaaabab; ch. 137: tibiotarsus, sulcus extensorius: medially situated (a), centrally situated (b) – scoring is ?bbbbaaa; ch 138: fourth toe with elongated phalanges: no (a), yes (b) – scoring is ?bbbbaaa; ch. 139: atlas, foramina transversaria: absent (a), present (b) – scoring is aabbbabb; ch. 140: pterygoid: facies articularis basipterygoidei centrally positioned and strongly protruding (a), rostrally positioned and weakly protruding (b), absent (c) – scoring is ?aaaabca; ch. 141: rami mandibularum: low, not very deep in caudal section (a), tall, very deep in caudal section (b) – scoring is bbbbbaaa.

The data were analysed with the heuristic search modus of PAUP*4.0a169 (Swofford, 2002). Outgroup comparisons were performed with the charadriiform Burhinidae.

SYSTEMATIC PALEONTOLOGY

Aves Linnaeus, 1758
Galloanseres (Sibley et al., 1988)
Danielsavidae, fam. nov.

zoobank.org/1815AD55-6C11-486D-8D48-DDD58A9D7639

Type genus. *Danielsavis* Houde et al., 2023.
Diagnosis. Galloanserine birds with a short, "galliform-like" beak, which are characterised by the combination of the following features: Palatine without angulus caudolateralis; mandible with flange-like process for the attachment of musculus adductor mandibulae externus; atlas with foramina transversaria (as in Anseranatidae and Anatidae); thoracic vertebrae with large pneumatic openings on lateral sides of corpus; coracoid with foramen nervi supracoracoidei and well-developed crista procoracoidei; humerus with wide proximal end; tibiotarsus with medially situated sulcus extensorius; phalanges of fourth toe, especially the third phalanx, short.
Differential diagnosis. Danielsavidae, fam. nov. is distinguished from the Anachronornithidae Houde et al., 2023 in that the tip of the upper beak is less

broadly rounded; the rami mandibularum of the lower jaw are less deep; the humerus is less elongated and has a broader proximal end (ratio length of bone to maximum proximal width 3.4 versus 4.1 in *Anachronornis anhimops*); the carpometacarpus lacks a proximocaudally projected trochlea carpalis; the trochlea metatarsi II is proportionally longer; and the phalanges of the fourth toe, especially the third phalanx, are proportionally shorter.

Danielsavis Houde et al., 2023
Danielsavis nazensis Houde et al., 2023

Holotype. NMS.Z.2021.40.1 (Figure 1A; partial skeleton including tip of upper beak, left and right mandibular rami, both quadrates and pterygoids, partial hyoid apparatus, at least 18 presacral vertebrae, cranial portion of sternum, partial furcula, right and partial left coracoid, cranial portions of both scapulae, left and distal end of right humerus, both radii, left ulna, ossa carpalia and wing phalanges, right and proximal portion of left carpometacarpus, distal end of right femur, proximal end of left and distal end of right tibiotarsus, right and distal end of left tarsometatarsus, pedal phalanges).
Referred specimens. NMS.Z.2021.40.2 (Figure 1B; partial skeleton including partial skull and mandible, both quadrates, partial hyoid apparatus, six cervical vertebrae, cranial portion of sternum, partial furcula, right coracoid, cranial portion of right scapula, proximal end of right humerus); NMS.Z.2021.40.3 (Figure 1C; partial skeleton including two cervical, two thoracic, and two caudal vertebrae, partial sternum, distal portion of left ulna, left radius, proximal end of right carpometacarpus, distal end of left femur, proximal and distal ends of right tarsometatarsus, and pedal phalanges); NMS.Z.2021.40.6 (Figure 1D; left tarsometatarsus, pedal phalanges).
Remarks. Houde et al. (2023) only considered the holotype to be definitely referable to *Danielsavis nazensis*. NMS.Z.2021.40.2 is slightly larger than the holotype, and according to Houde et al. (2023: 32), the specimen differs from the holotype "because in lateral view the orbital process of the quadrate is narrower and the dorsal margin of the quadrate between it and the otic process is more uniformly curved. The premaxilla is slightly longer and narrower than that of *Danielsavis nazensis* (…). The tubercle of the external head of the AME [= (musculus) adductor mandibulae externus], pars articularis is positioned closer to the dorsal margin of the coronoid region". Unlike in the holotype (NMS.Z.2021.40.1), the quadrate of NMS.Z.2021.40.2 furthermore exhibits a well-defined albeit small condylus pterygoideus and the

FIGURE 1. Overview of the main bones preserved in the specimens of *Danielsavis nazensis* Houde et al., 2023 from the London Clay of Walton-on-the-Naze (Essex, UK). **A,** holotype, NMS.Z.2021.40.1 (not shown are the radii, which were figured by Houde et al., 2023: figure 5Q, R). **B,** referred specimen NMS.Z.2021.40.2 (the two separate blocks of matrix containing the beak and the neurocranium, respectively, were assembled for the photo; not shown is the cranial portion of the sternum, which was figured by Houde et al., 2023: figure 7E, F). **C,** referred specimen NMS.Z.2021.40.3. **D,** referred specimen NMS.Z.2021.40.6. **Abbreviations:** for, foramen piercing skull roof; wdn, widening of scapus claviculae. The scale bars equal 10 mm.

scapula of the holotype is proportionally longer and narrower than in NMS.Z.2021.40.2. Some of these differences may be due to the somewhat larger size of NMS.Z.2021.40.2, and we consider it possible that they are due to intraspecific variation.

With regard to NMS.Z.2021.40.3, Houde et al. (2023: 34) noted that the "alular metacarpal of the carpometacarpus is extremely short proximodistally and positioned proximally, such that the distal limits of the alular process and the pisiform process

are approximately equal, unlike the holotype of *Danielsavis nazensis*". However, the os metacarpale alulare of NMS.Z.2021.40.3 is broken and was glued together by the collector, so that this difference is likely to be an artefact of an erroneous restoration of the bone.

Emended description. In the following, we focus on features that were not already mentioned by Houde et al. (2023). The upper beak of *Danielsavis* (Figure 2A–D) has a distinctive shape in that its lat-

eral margins run in parallel and in that the tip is not deflected and does not form a hook. Even though it resembles the upper beak of *Anhima cornuta* (Anhimidae) in its outline, the straight tomia distinguish it from crown group Anhimidae. The beak of *Anachronornis* has a more spatulate shape with a broadly rounded tip; the nostrils are proportionally longer than in *Danielsavis*. Mayr (2022) considered the beak of *Danielsavis* to be similar to that of *Asteriornis* from the Late Cretaceous of Belgium (Field et al., 2020), but in spite of a similar outline it is proportionally shorter; the interorbital section of the neurocranium is wider than in *Asteriornis* and *Anachronornis*. As noted by Houde et al. (2023), the lacrimals appear to be co-ossified with the frontals; on the right side of the skull, there is a small foramen that pierces the skull roof in the presumed area of fusion (Figure 1B), but it is uncertain whether this is a true osteological feature or the result of damage (a similar foramen is also present in some extant anseriforms with co-ossified lacrimals, such as *Cairina moschata*).

Specimen NMS.Z.2021.40.2 preserves the basicranial area and substantial portions of both palatine bones (Figure 2E–G), which were not described by Houde et al. (2023). The right basipterygoid process is visible, being sessile and of ovate shape as in extant galloanserines. The morphology of the palatines is intermediate between that of crown group Galliformes and crown group Anseriformes. As in *Anachronornis* and galliforms, but unlike in crown group Anseriformes, the caudal portions of the palatines are not co-ossified. The crista ventralis is low and separates the bone into two portions of subequal width (pars lateralis and lamella dorsalis, pars choanalis palatini *sensu* Zusi and Livezey, 2006). The pars lateralis is mediolaterally wider than in crown group Galliformes (Figure 2H), but as in the latter and unlike in crown group Anseriformes (Figure 2I, J), the lateral margin of the palatine is evenly curved and does not form a well-defined angulus caudolateralis (the condition in *Anachronornis* is similar to that of *Danielsavis*).

The quadrate (Figure 3A–H) was figured by Houde et al. (2023), who noted some galloanserine features of the bone in the differential diagnosis and commented on the presence of a foramen pneumaticum basiorbitale; this foramen is absent or vestigial (some Anhimidae) in crown group Anseriformes (Elzanowski and Stidham, 2010). As in other galloanserine birds, the processus mandibularis is bicondylar and lacks a condylus caudalis. In its proportions and general features, the

quadrate of *Danielsavis* corresponds well to that of *Presbyornis*, which likewise exhibits a more plesiomorphic quadrate morphology than crown group Anseriformes (Elzanowski and Stidham, 2010). The tuberculum subcapitulare is distinct but small. The processus orbitalis is proportionally longer and narrower than in *Anachronornis*. In NMS.Z.2021.40.1, a well-defined condylus pterygoideus is absent, whereas this condyle is very small in NMS.Z.2021.40.2; a small prominence on the processus orbitalis may represent an articulation facet for the pterygoid. The cotyla quadratojugalis exhibits a facies quadratojugalis ventralis *sensu* Elzanowski and Stidham (2010).

Both pterygoids are present in the holotype (Figure 3O–R). The bones were not described by Houde et al. (2023) and – except for the shorter processus rostralis – most closely resemble the pterygoid of *Nettapterornis ("Anatalavis") oxfordi* in overall proportions (compare Figure 3O–R with Olson, 1999: figure 3). As in the latter species, the facies articularis basipterygoidea is proportionally wider than in crown group Anseriformes (Figure 3K, L). The pterygoid of *Danielsavis* is clearly distinguished from the pterygoid of galliform birds (Figure 3I, J), in which the facies articularis basipterygoidei is less protruding and situated near the rostral end of the bone.

The hyoid apparatus (Figure 3S–U), which was likewise not described by Houde et al. (2023), has a wide basihyal, which tapers rostrally and forms lateral wing-like projections. Within extant Galloanseres a similar morphology occurs in the Anseranatidae (Figure 3X), whereas the basihyal of the Anhimidae (Figure 3W) and Galliformes (Figure 3V) is narrow and rod-shaped. A small, subrectangular ossicle is here tentatively identified as the os paraglossum (Figure 3U); if this identification is correct, the bone is distinctly smaller than the paraglossum of crown group Anseriformes.

The caudal (articular) end of the mandible (Figure 2K–P) exhibits the characteristic derived morphology of galloanserine birds, in which a rostrocaudal ridge separates two articular surfaces for the quadrate. As in other Galloanseres, a long processus retroarticularis is present, which is completely preserved in the left mandibular ramus of the holotype. The processus retroarticularis of *Danielsavis* is sharply dorsally angled, by which it differs from *Anachronornis* (Figure 2R). The mandibular rami are dorsoventrally lower than in *Asteriornis, Anachronornis, Presbyornis,* and all crown group Anseriformes and agree with the mandibular rami of galliform birds in their proportions. This is
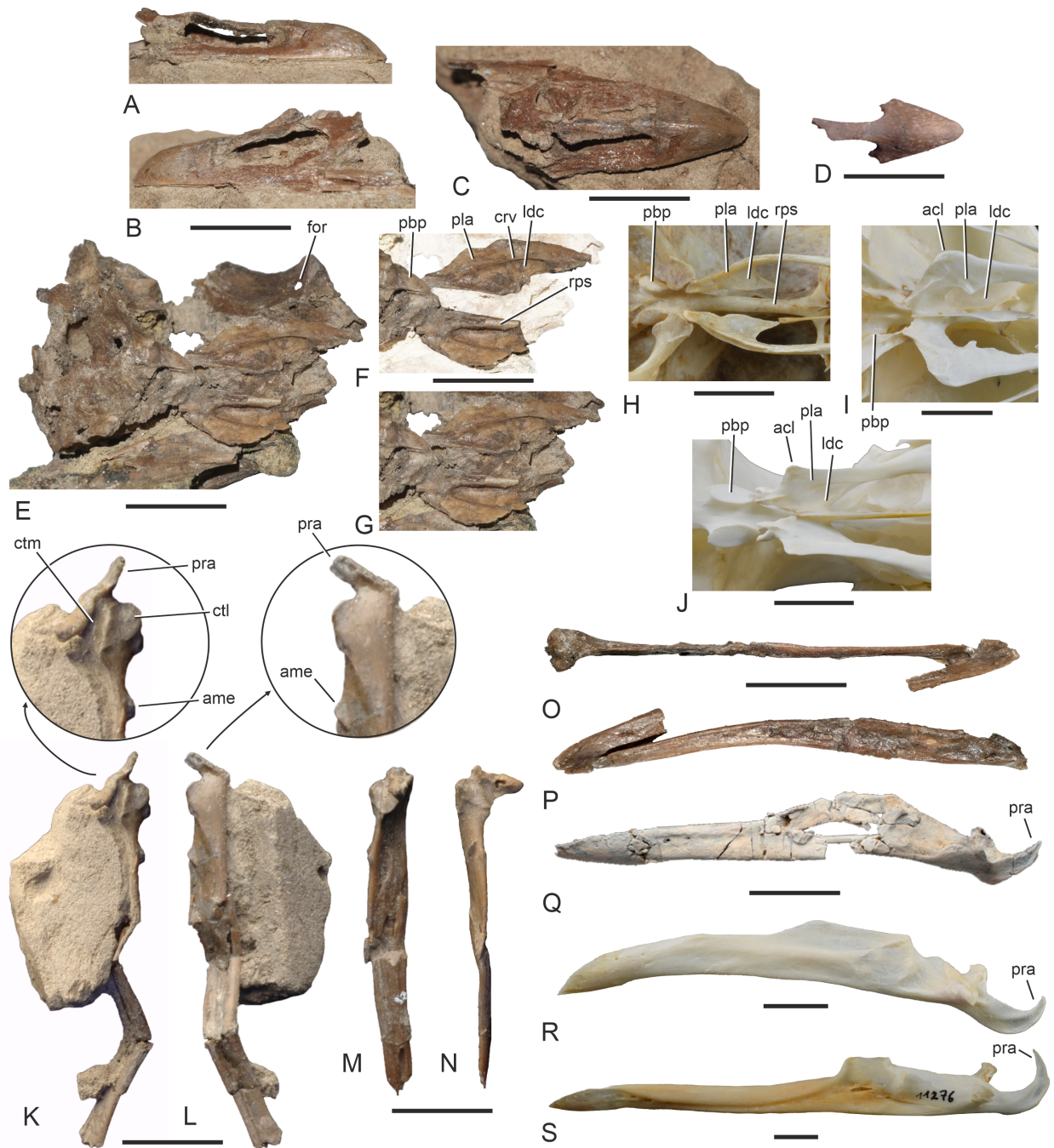
FIGURE 2 (caption on next page).

also true for the short symphysis, which is medio-laterally narrower than the mandibular symphysis of crown group Anseriformes. On the lateral surface of the mandibular ramus there is an elongated, flange-like process that served for the attachment of musculus adductor mandibulae externus ("tubercle of the external head of the AME, pars articularis" *sensu* Houde et al., 2023:

32). A similar flange is present in the Megapodiidae, but absent in other crown group Galliformes (Cracidae and Phasianidae); in crown group Anseriformes it is weakly developed in the Anhimidae and very pronounced in the Anseranatidae and Anatidae.

The holotype includes at least 18 presacral vertebrae or fragments thereof, with this vertebral

FIGURE 2 (figure on previous page). *Danielsavis nazensis* Houde et al., 2023, upper beak, palate, and mandible. **A–C,** *D. nazensis*, upper beak of NMS.Z.2021.40.2 in right lateral (**A**), left lateral (**B**), and dorsal (**C**) view. **D,** *D. nazensis*, tip of the upper beak of the holotype (NMS.Z.2021.40.1) in dorsal view. **E,** *D. nazensis*, neurocranium of NMS.Z.2021.40.2 in ventral view. **F, G,** *D. nazensis*, palatine bones of NMS.Z.2021.40.2 in ventral view, in **F,** surrounding bones and matrix were digitally brightened. **H–J,** palatines (ventral view) of **H,** *Alectura lathami* (Megapodiidae, Galliformes; SMF 7243); **I,** *Chauna torquata* (Anhimidae, Anseriformes; SMF 19920); **J,** *Anseranas semipalmata* (Anseranatidae, Anseriformes; SMF 11276). **K, L,** *D. nazensis*, left ramus mandibulae of the holotype (NMS.Z.2021.40.1) in dorsal (**K**) and lateral (**L**) view; the arrows denote details of the caudal end. **M, N,** *D. nazensis*, right ramus mandibulae of the holotype (NMS.Z.2021.40.1) in medial (**M**) and dorsal (**N**) view. **O, P,** *D. nazensis*, partial mandible of NMS.Z.2021.40.2 in dorsal (**O**) and dorsolateral (**P**) view; the arrow denotes a detail of the caudal end. **Q,** mirrored right ramus mandibulae of *Anachronornis anhimops* from the late Paleocene of Wyoming (holotype, coated with ammonium chloride; from Houde et al., 2023: figure 1, published under a CC BY 4.0 license). **R,** mandible of *C. torquata* (SMF 19920) in lateral view. **S,** mandible of *A. semipalmata* (SMF 11276) in lateral view. **Abbreviations:** acl, angulus caudolateralis; ame, flange-like process that served for the attachment of musculus adductor mandibulae externus; crv, crista ventralis; ctl, cotyla lateralis; ctm, cotyla medialis; for, foramen piercing skull roof; ldc, lamella dorsalis, pars choanalis palatini; pbp, processus basipterygoideus; pla, pars lateralis; pra, processus retroarticularis; rps, rostrum parasphenoidale. The scale bars equal 10 mm.

series being complemented by vertebrae preserved in NMS.Z.2021.40.2 and NMS.Z.2021.40.3. Houde et al. (2023) commented on the morphology of the atlas, which exhibits foramina transversaria (Figure 4A); in extant Galloanseres, these foramina occur in the Anseranatidae and Anatidae (Figure 4C), whereas they are absent in the Anhimidae (Figure 4B) and Galliformes (Figure 4D). As further noted by Houde et al. (2023), the thoracic vertebrae bear large pneumatic openings on the lateral surfaces of the corpus (Figure 4E); these openings are present in anseriforms but absent in galliforms (Mayr, 2021). Other vertebrae were not described by Houde et al. (2023). The axis, which is present in NMS.Z.2021.40.2 (Figure 4E, F), is proportionally shorter than that of *Conflicto* and in its shape resembles the axis of *Chauna* (Anhimidae; Figure 4B, G); it bears a long and ridge-like processus spinosus. In their proportions, the third to fifth cranial vertebrae are more similar to the corresponding vertebrae of crown group Anseriformes than to the wider vertebrae of crown group Galliformes. The third and fourth cervicals (Figure 4A, J, K) exhibit a small notch (third) or foramen (fourth) on one side of the corpus, but these are much smaller than the foramina in the corresponding vertebrae of galliforms and some anseriforms. The large processus ventralis of the third vertebra is pierced by foramina (Figure 4K). The vertebra that is here identified as the fifth cervical is only preserved in NMS.Z.2021.40.3 (Figure 4A); it is much longer than wide and has a caudally tapering corpus; a lateral lamella along its corpus delimits a foramen in the cranial portion of the vertebra. The lateral surfaces of the corpus of some cervical vertebrae bear small, irregular and lamellate projections (Figure 4E), which are fewer and less pronounced than

the barb-like tubercles in the fossils we refer to *Perplexicervix* (see further below). One of the thoracic vertebrae preserved in NMS.Z.2021.40.3 exhibits ossified tendons attached to the processus spinosus and the zygapophysis caudalis (Figure 4L); a long processus ventralis identifies this vertebra as one of the cranial thoracics. The pygostyle is preserved in the holotype and has a craniocaudally wide lamina; the dorsal portion of the lamina pygostyli is broadly rounded.

The coracoid of *Danielsavis* (Figure 5A, B) differs from that of *Anachronornis* (Figure 5D) and other anseriforms (Figure 5E, F) in that the crista procoracoidei is more strongly developed, the omal extremity proportionally shorter, and the angle between the medio-omal and latero-omal portions of the processus acrocoracoideus is more obtuse. With regard to the shape of the processus acrocoracoideus, the bone resembles the coracoid of early Paleogene stem group Galliformes (Figure 5C). The facies articularis clavicularis does not form a lip-like projection and the impressio ligamenti acrocoracohumeralis is not as marked as in *Anachronornis* and other anseriforms. The facies articularis humeralis is more laterally facing than in *Anachronornis*, in which it is more dorsally directed. The foramen nervi supracoracoidei is large. The medial margin of the extremitas sternalis forms a small projection, which is also found in other fossil Galloanseres. The processus lateralis is less drawn in sternolateral direction than in *Anachronornis* and *Nettapterornis* (Figure 5E). Houde et al. (2023: 29) noted the presence of potential pneumatic foramina on the dorsal surface of the extremitas sternalis of NMS.Z.2021.40.1, but we consider these foramina to more likely be artefacts of damage to the bones.
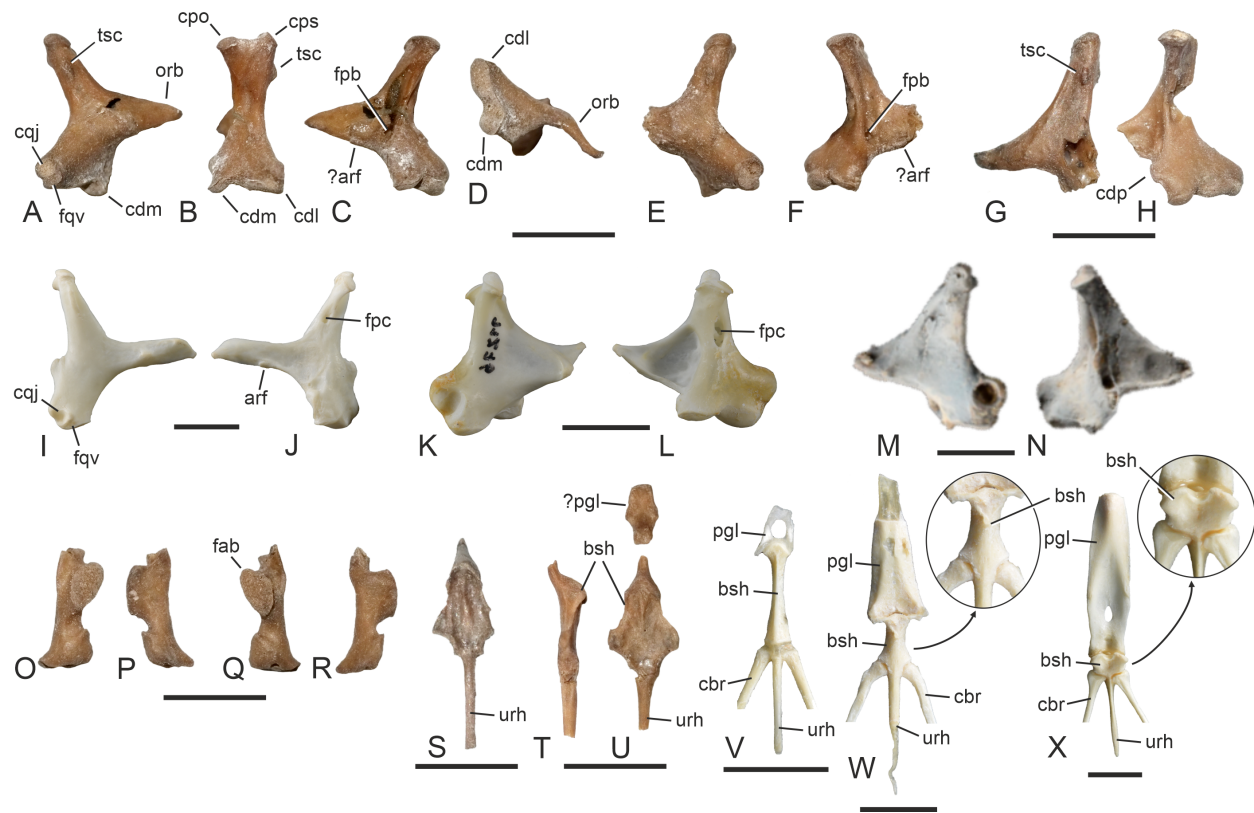
FIGURE 3. Cranial elements and hyoid bone of *Danielsavis nazensis* Houde et al., 2023 in comparison with those of other galloanserine birds. **A–F,** *D. nazensis* (holotype, NMS.Z.2021.40.1), right (**A–D**) and left (**E, F**) quadrate in lateral (**A, E**), caudal (**B**), medial (**C, F**), and ventral (**D**) view. **G, H,** *D. nazensis* (NMS.Z.2021.40.2), left (**G**) and right (**H**) quadrate in lateral view. **I, J,** right quadrate of *Pipile jacutinga* (Cracidae, Galliformes; SMF 4139) in lateral (**I**) and medial (**J**) view. **K, L,** mirrored left quadrate of *Anseranas semipalmata* (Anseranatidae, Anseriformes; SMF 11276) in lateral (**K**) and medial (**L**) view. **M, N,** *Anachronornis anhimops* from the late Paleocene of Wyoming (holotype, coated with ammonium chloride; from Houde et al., 2023: figure 1, published under a CC BY 4.0 license), left quadrate in lateral (**M**) and medial (**N**) view. **O–R,** *D. nazensis* (holotype, NMS.Z.2021.40.1), right (**O, P**) and left (**Q, R**) pterygoid in dorsal (**O, Q**) and medial (**P, R**) view. **S,** *D. nazensis* (NMS.Z.2021.40.2), basiurohyal in dorsal view. **T, U,** *D. nazensis* (holotype, NMS.Z.2021.40.1), basiurohyal and putative paraglossum in lateral (**T**) and dorsal (**U**) view. **V,** *Alectura lathami* (Megapodiidae, Galliformes; SMF 19785), basiurohyal and paraglossum in dorsal view. **W,** *Chauna torquata* (Anhimidae, Anseriformes; SMF 19920), basiurohyal and paraglossum in dorsal view; the arrow denotes an enlarged detail of the basihyal. **X,** *A. semipalmata* (SMF 19902), basiurohyal and paraglossum in dorsal view; the arrow denotes an enlarged detail of the basihyal. **Abbreviations:** arf, articular facet for pterygoid; bsh, os basihyale; cbr, os ceratobranchiale; cdl, condylus lateralis; cdm, condylus medialis; cdp, condylus pterygoideus; cpo, capitulum oticum; cps, capitulum squamosum; cqj, cotyla quadratojugalis; fab, facies articularis basipterygoidea; fpb, foramen pneumaticum basiorbitale; fpc, foramen pneumaticum caudomediale; fqv, facies quadratojugalis ventralis; orb, processus orbitalis; pgl, os paraglossum; tsc, tuberculum subcapitulare; urh, os urohyale. The scale bars equal 5 mm.

Unlike in galliform birds, the extremitas omalis of the furcula (Figure 5G) forms a well-developed processus acromialis (in galliform birds the omal extremity is widened and has a straight end). The apophysis furculae is small. The scapus claviculae of NMS.Z.2021.40.2 exhibits an unusual mediolateral widening in its omal portion (Figure 1B), which may represent a pathological feature. The scapula has a long and narrow acromion, similar to that of the putative presbyornithid *Wilaru tedfordi* from the late Oligocene of Australia (De Pietri et al., 2016: figure 1g).

The humerus (Figure 5L, M) is notably stouter than that of *Anachronornis* and anseriforms (Figure 5N, O) and has a proportionally wider proximal end. The tuberculum dorsale is proximodistally longer than it is mediolaterally wide and is proportionally longer than in *Anachronornis* and crown group anseriforms. On the distal end of the bone, the pro-
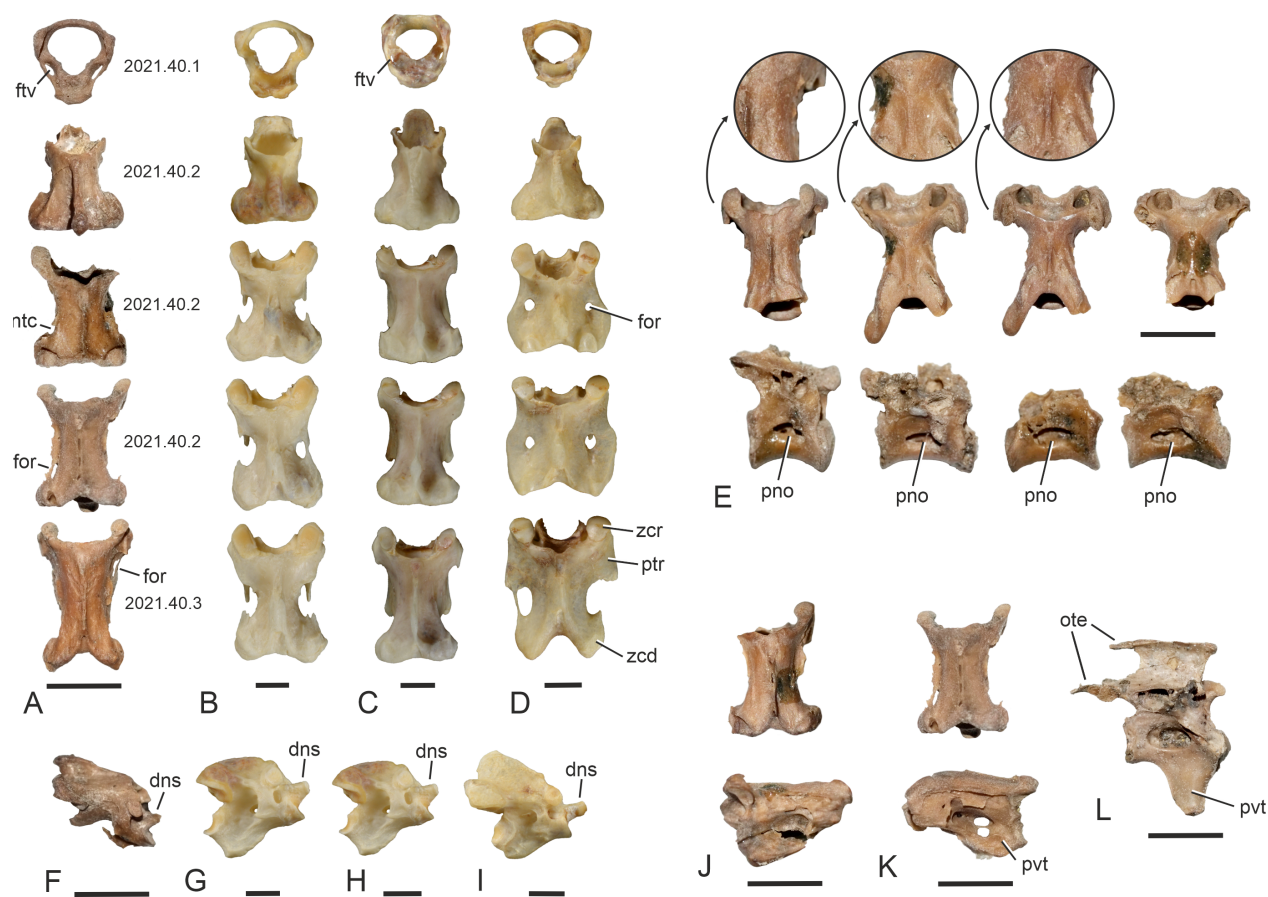
FIGURE 4. *Danielsavis nazensis* Houde et al., 2023, comparison of the vertebrae with those of other galloanserine birds. **A,** *D. nazensis*, cranialmost five cervical vertebrae (atlas: NMS.Z.2021.40.1; axis, third, and fourth vertebra: NMS.Z.2021.40.2; fifth vertebra: NMS.Z.2021.40.3). **B–D,** cranialmost five cervical vertebrae of **B,** *Chauna torquata* (Anhimidae, Anseriformes; SMF 11885); **C,** *Dendrocygna arborea* (Anatidae, Anseriformes; SMF 6591); **D,** *Alectura lathami* (Megapodiidae, Galliformes; SMF 7243). **E,** *D. nazensis*, selected cervical and thoracic vertebrae of the holotype (NMS.Z.2021.40.1); the arrows denote enlarged details of the bones to show irregular lamellate projections. **F–I,** axis in lateral view of **F,** *D. nazensis* (NMS.Z.2021.40.2); **G,** *C. torquata* (SMF 11885); **H,** *D. arborea* (SMF 6591); **I,** *A. lathami* (SMF 7243). **J,** *D. nazensis*, fourth cervical vertebra of the holotype (NMS.Z.2021.40.1) in dorsal and lateral view. **K,** *D. nazensis*, fourth cervical vertebra of the referred specimen NMS.Z.2021.40.2 in dorsal and lateral view. **L,** *D. nazensis*, thoracic vertebra in lateral view (NMS.Z.2021.40.3). **Abbreviations:** dns, dens; for, foramen; ftv, foramen transversarium; ntc, notch; ote, ossified tendons; pno, pneumatic opening; ptr, processus transversus; pvt, processus ventralis; zcd, zygapophysis caudalis; zcr, zygapophysis cranialis. The scale bars equal 5 mm.

cessus flexorius is more developed than in *Anachronornis* and other anseriforms.

The proximal end of the ulna (Figure 5R) closely agrees with that of galliform birds (Figure 5S), and as in the latter the cotyla dorsalis reaches much farther distally than the cotyla ventralis. The carpometacarpus (Figure 5U, V) has a proportionally wider spatium intermetacarpale than the carpometacarpus of *Anachronornis* (Figure 5X) and other anseriforms. Furthermore, unlike in *Anachronornis, Nettapterornis* (Figure 5W) and crown group Anseriformes, the trochlea carpalis is not proximocaudally projected.

The phalanx proximalis digiti majoris exhibits a processus internus indicis. The os carpi radiale (Figure 5Y, Z) corresponds to that of anseriforms (Figure 5AA), whereas the corresponding ossicle of crown group galliforms has a disparate, autapomorphic shape (Figure 5BB).

The tibiotarsus (Figure 6A) differs from that of crown group anseriforms in that the sulcus extensorius is medially rather than centrally situated. The condylus medialis is much narrower than the condylus lateralis. Only a fragment of the proximal end is preserved in the holotype, which shows cristae cnemiales of average size.
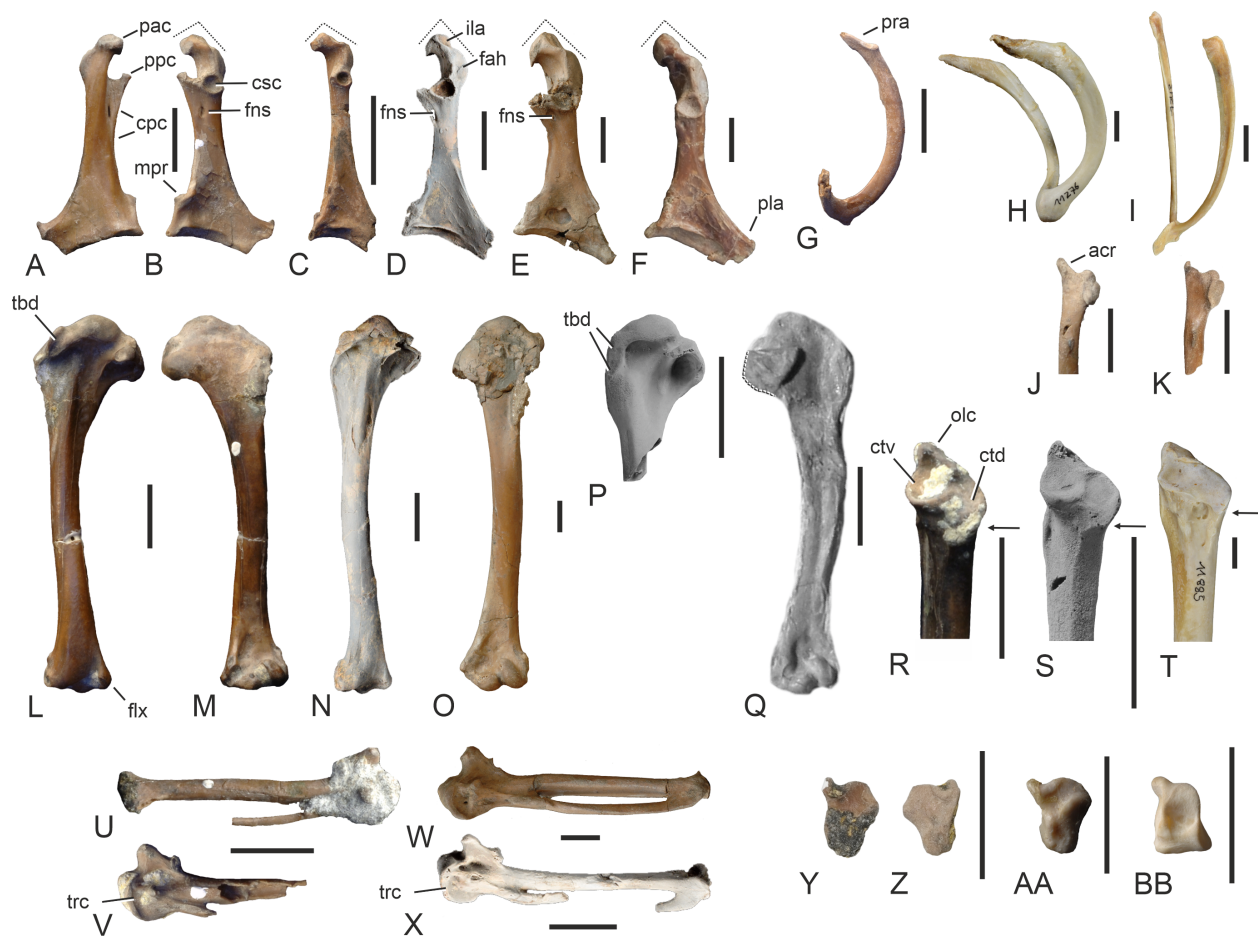
FIGURE 5 (caption on next page).

The tarsometatarsus (Figure 6F–J) is proportionally shorter than the tarsometatarsus of the Anhimidae. Unlike in crown group Anseriformes, the plantar articular surface of the trochlea metatarsi III is asymmetrical, with a more proximal lateral rim (Figure 6J). In contrast to *Anachronornis* (Figure 6N), the trochlea metatarsi II is not much shorter than the trochlea metatarsi IV. The hypotarsus was described by Houde et al. (2023: 30) as showing "a single deep sulcus", but in specimen NMS.Z.2021.40.3 there are two shallow sulci, presumably for the tendons of m. flexor digitorum longus and m. flexor hallucis longus (Figure 6E). In proximal view the hypotarsus corresponds to that of *Presbyornis* (De Pietri et al., 2016: figure 2d').

The os metatarsale I is characterised by a deep incision in the distal portion of the trochlea. The pedal phalanges (Figure 6K) correspond to those of galliform birds in their proportions, and especially those of the fourth toe are much shorter than the corresponding phalanges of most anseriform birds (exceptions are the taxa *Cnemiornis* and *Cereopsis*, in which equally short phalanges occur), with the third phalanx of the fourth toe being particularly short. Houde et al. (2023) hypothesised that the longest phalanx represented in the phalangeal set is from the hallux, but we consider this phalanx to be the first phalanx of the second toe. The first phalanx of the hallux, which is identified by the asymmetrical shape of its proximal end, is rather shorter.

cf. Otidiformes Wagler, 1830
Perplexicervicidae, fam. nov.

zoobank.org/DD21066A-8B29-4189-AB41-29945747EF21

Type genus. *Perplexicervix* Mayr, 2010.
Diagnosis. Skull with stalked processus basipterygoidei (Mayr, 2007); surfaces of cervical vertebrae covered with numerous barb-like tubercles; thoracic vertebrae with large pneumatic openings on lateral surfaces of corpus; coracoid (according to the tentatively referred specimens described in the present study) with deeply excavated cotyla scapularis and foramen nervi supracoracoidei.

FIGURE 5 (figure on previous page). *Danielsavis nazensis* Houde et al., 2023, comparison of pectoral girdle and wing bones with those of other galloanserine birds. **A, B,** *D. nazensis* (holotype, NMS.Z.2021.40.1), right coracoid in ventral (**A**) and dorsal (**B**) view. **C,** right coracoid of an undescribed stem group galliform from Walton-on-the-Naze in dorsal view. **D,** mirrored left coracoid of *Anachronornis anhimops* from the late Paleocene of Wyoming (holotype, coated with ammonium chloride; from Houde et al., 2023: figure 2, published under a CC BY 4.0 license) in dorsal view. **E,** right coracoid of *Nettapterornis oxfordi* from Walton-on-the-Naze (holotype, NHMUK A 5922) in dorsal view. **F,** mirrored left coracoid of the presbyornithid *Telmabates antiquus* from the early Eocene of Argentina (AMNH 3181). **G,** partial furcula of *D. nazensis* (NMS.Z.2021.40.2) in craniomedial view. **H,** furcula of *Anseranas semipalmata* (Anseranatidae, Anseriformes; SMF 11276) in caudomedial view. **I,** furcula of *Alectura lathami* (Megapodiidae, Galliformes; SMF 7243) in caudomedial view. **J, K,** cranial extremity of right scapula of *D. nazensis* (**J:** holotype, NMS.Z.2021.40.1; **K:** NMS.Z.2021.40.2) in lateral view. **L, M,** left humerus of *D. nazensis* (holotype, NMS.Z.2021.40.1) in caudal (**L**) and cranial (**M**) view. **N,** left humerus of *A. anhimops* (holotype, coated with ammonium chloride; from Houde et al., 2023: figure 2, published under a CC BY 4.0 license) in caudal view. **O,** left humerus of *N. oxfordi* (holotype, NHMUK A 5922) in cranial view. **P,** mirrored proximal end of a right humerus from the early Eocene of Egem in Belgium (IRSNB Av 163); coated with ammonium chloride. **Q,** left humerus of *Gallinuloides wyomingensis* from the early Eocene Green River Formation (Wyoming, USA; WDC CGR−012) in cranial view; surrounding matrix was digitally removed, the dotted line indicates the reconstructed outline of the ventral portion of the proximal end. **R–T,** proximal end of left ulna in cranial view of **R,** *D. nazensis* (holotype, NMS.Z.2021.40.1); **S,** an unnamed galliform from the early Eocene of Egem in Belgium (IRSNB Av 164); **T,** *Chauna torquata* (Anhimidae, Anseriformes; SMF 11885); the arrows point to the distal end of the cotyla dorsalis. **U, V,** *D. nazensis* (holotype, NMS.Z.2021.40.1), right (**U**) and proximal left (**V**) carpometacarpus in ventral view. **W,** *N. oxfordi* (holotype, NHMUK A 5922), left carpometacarpus in ventral view. **X,** *A. anhimops* (holotype, coated with ammonium chloride; from Houde et al., 2023: figure 2, published under a CC BY 4.0 license), left carpometacarpus in ventral view. **Y, Z,** *D. nazensis* (holotype, NMS.Z.2021.40.1), left (**Y**) and right (**Z**) os carpi radiale in cranial view. **AA,** *Dendrocygna viduata* (Anatidae, Anseriformes; SMF 2418), left os carpi radiale in cranial view. **BB,** *Pternistis squamatus* (Phasianidae, Galliformes; SMF 10151), left os carpi radiale in cranial view. The dotted lines in **B–F** indicate the angle between the medio-omal and latero-omal portions of the processus acrocoracoideus. **Abbreviations:** acr, acromion; cpc, crista procoracoidei; csc, cotyla scapularis; ctd, cotyla dorsalis; ctv, cotyla ventralis; fah, facies articularis humeralis; flx, processus flexorius; fns, foramen nervi supracoracoidei; ila, impressio ligamenti acrocoracohumeralis; mpr, medial projection; olc, olecranon; pac, processus acrocoracoideus; pla, processus lateralis; ppc, processus procoracoideus; pra, processus acromialis; tbd, tuberculum dorsale; trc, trochlea carpalis. The scale bars equal 10 mm.

Perplexicervix Mayr, 2010
Perplexicervix paucituberculata, sp. nov.

zoobank.org/0A8FEDE9-3FBD-4DFE-8609-64E1D4F57D55

Holotype. NMS.Z.2021.40.7 (Figure 7A; partial skeleton including fragment of left and right otic regions of skull, caudal end of jugal bar, elements of the hyoid apparatus, 15 presacral vertebra, 6 caudal vertebrae, pygostyle).

Differential diagnosis. Differs from *Perplexicervix microcephalon* in that covering of vertebrae with tubercles less extensive; scapula of tentatively referred specimen with more strongly ventrally protruding facies articularis humeralis. Distinguished from *Danielsavis nazensis* in that atlas lacks foramina transversaria, axis proportionally shorter, cervical vertebrae with tuberculate surface, basihyal rod-shaped, pygostyle proportionally larger (the tentatively referred coracoid and humerus are altogether different from the corresponding bones of *Danielsavis*).

Etymology. The species epithet is derived from paucis (Lat.): little and tuberculatus (Lat.): tuberculate, in reference to the fact that the surfaces of the vertebrae are less tuberculate than in *P. microcephalon* from Messel.

Type locality and horizon. Walton-on-the-Naze, Essex, United Kingdom; Walton Member of the London Clay Formation (previously Division A2; Jolley, 1996; Rayner et al., 2009; Aldiss, 2012); early Eocene (early Ypresian, 54.6–55 Ma; Collinson et al., 2016).

Tentatively referred specimens. NMS.Z.2021.40.91 (Figure 7B; partial skeleton including left coracoid, cranial extremities of both scapulae, partial furcula, proximal and distal ends of left humerus, partial right humerus, proximal portion of radius, proximal end of right ulna); collected in 1991 by M. Daniels (original collector's number WN 91699). NMS.Z.2021.40.92 (Figure 7C; partial skeleton including right coracoid, cranial extremities of both scapulae, fragment of cranial portion of sternum, proximal and distal portions of right humerus, distal portion of left humerus in piece of matrix, distal end of left ulna, left carpometacarpus, left and right os carpi ulnare, left os carpi radiale, phalanges of left wing); collected in 1991 by M. Daniels (original collector's number WN 91712).
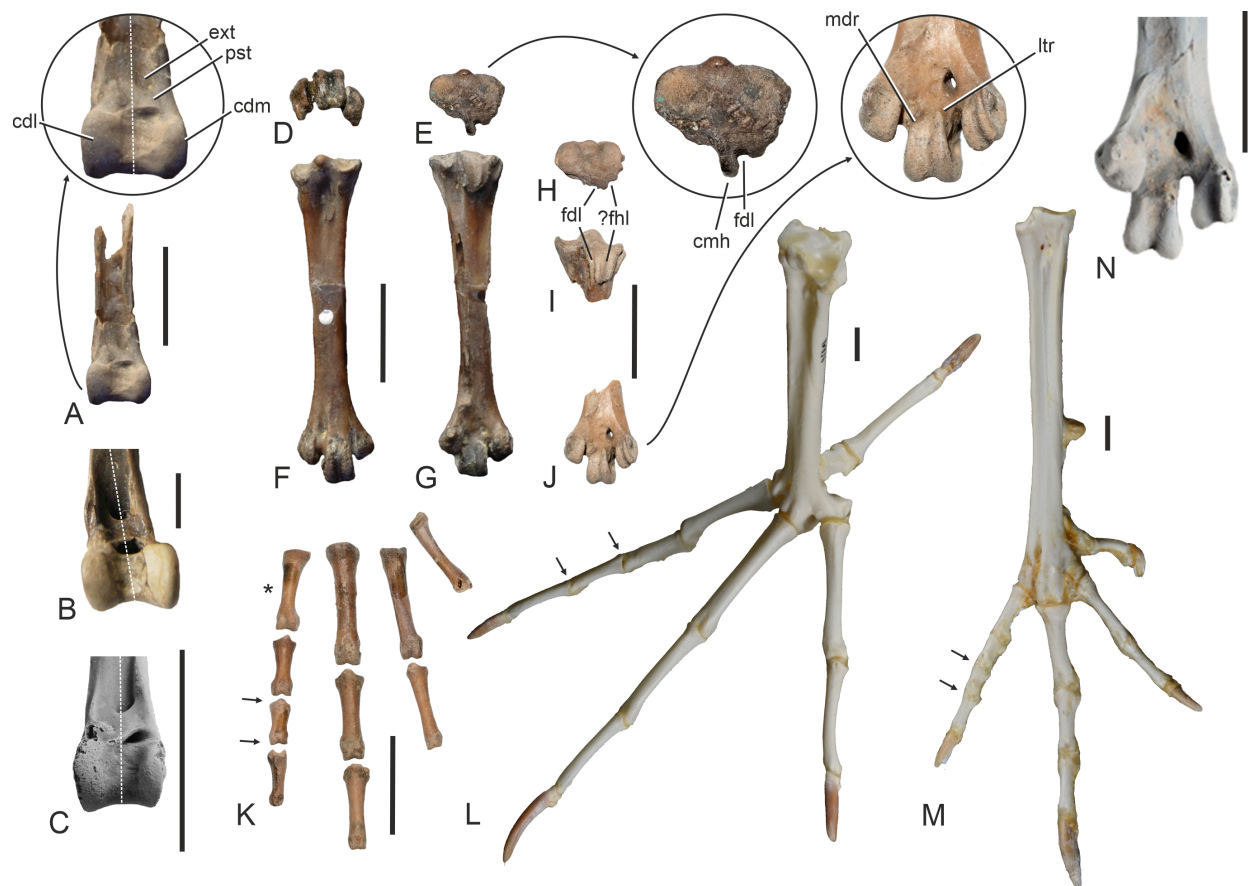
FIGURE 6. *Danielsavis nazensis* Houde et al., 2023, comparison of tibiotarsus, tarsometatarsus, pedal phalanges with other galloanserine birds. **A,** *D. nazensis* (holotype, NMS.Z.2021.40.1), distal end of right tibiotarsus; the arrow denotes an enlarged detail of the bone. **B,** distal end of right tibiotarsus of the anseriform *Saintandrea chenoides* from the late Oligocene of France (holotype, NMB Mar. 874e). **C,** mirrored distal end of left tibiotarsus of an unnamed galliform from the early Eocene of Egem in Belgium (IRSNB Av 168); coated with ammonium chloride. **D–G,** *D. nazensis* (holotype, NMS.Z.2021.40.1), right tarsometatarsus in distal (**D**), proximal (**E**), dorsal (**F**), and plantar (**G**) view; the arrow denotes an enlarged detail of the proximal end of the bone. **H, I,** *D. nazensis* (NMS.Z.2021.40.3), proximal end of right tarsometatarsus in proximal (**H**) and plantar (**I**) view. **J,** *D. nazensis* (NMS.Z.2021.40.3), distal end of right tarsometatarsus in plantar view; the arrow denotes an enlarged detail of the bone. **K,** *D. nazensis* (holotype, NMS.Z.2021.40.1), non-ungual pedal phalanges; the asterisk indicates a mirrored phalanx. **L,** mirrored left foot of *Chauna torquata* (Anhimidae, Anseriformes; SMF 19920). **M,** right foot of *Pavo cristatus* (Phasianidae, Galliformes; SMF 20342). **N,** mirrored distal end of left tarsometatarsus of *Anachronornis anhimops* (holotype, coated with ammonium chloride; from Houde et al., 2023: figure 2, published under a CC BY 4.0 license) in plantar view. The dotted lines in **A–C** indicate the midline of the distal tibiotarsus. The arrows in **K–M** denote the length of the third phalanx of the fourth toe. **Abbreviations:** cdl, condylus lateralis; cdm, condylus medialis; cmh, crista medialis hypotarsi; ext, sulcus extensorius; fdl, sulcus for musculus flexor digitorum longus; fhl, sulcus for musculus flexor hallucis longus; ltr, lateral rim of plantar articular surface of trochlea metatarsi III; mdr, medial rim of plantar articular surface of trochlea metatarsi III; pst, pons supratendineus. The scale bars equal 10 mm.

Measurements (maximum length, in mm). NMS.Z.2021.40.91: left coracoid 41.4.

Remarks. There is no overlap in the bones preserved in the holotype and the tentatively referred specimens NMS.Z.2021.40.91 and NMS.Z.2021.40.92, but as far as comparisons are possible the major skeletal elements preserved in the latter two specimens agree well with those of *P.* *microcephalon* from Messel (Figure 8). Comparisons with extant Otidiformes show the vertebrae of the holotype to correspond in size with the tentatively referred postcranial bones (Figure 9), and there are no other fossils in the Daniels collection that are of corresponding size and may have had tuberculate vertebrae (i.e., the cervicals are known
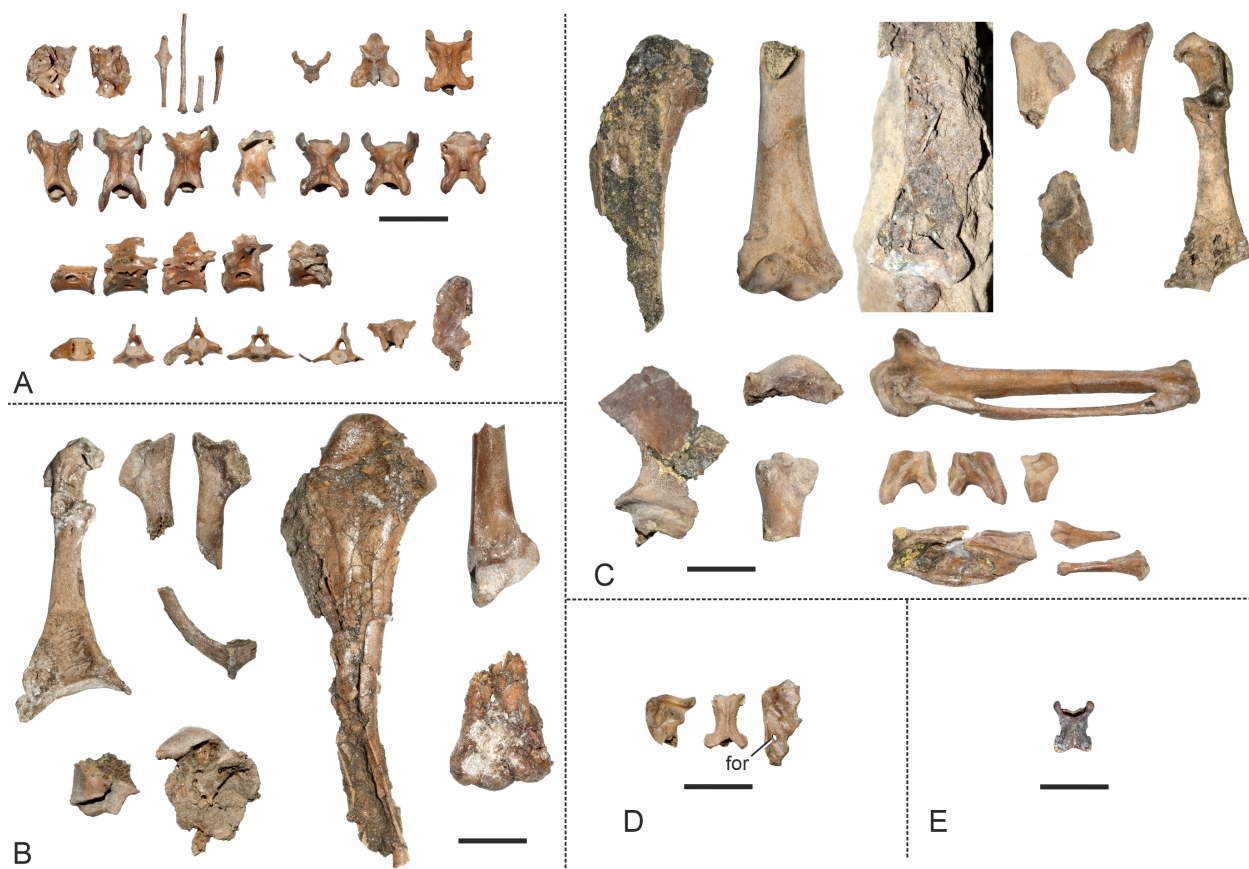
FIGURE 7. Specimens of *Perplexicervix paucituberculata*, sp. nov. and *Perplexicervix* sp. from the early Eocene London Clay of Walton-on-the-Naze (Essex, UK). **A,** *P. paucituberculata*, sp. nov. (holotype, NMS.Z.2021.40.7). **B,** cf. *P. paucituberculata*, sp. nov. (NMS .Z.2021.40.91). **C,** cf. *P. paucituberculata*, sp. nov. (NMS.Z.2021.40.92). **D,** *Perplexicervix* sp. (NMS.Z.2021.40.9). **E,** *Perplexicervix* sp. (NMS.Z.2021.40.10). **Abbreviation:** for, foramen perforating caudoventral portion of corpus pygostyli. The scale bars equal 10 mm.

from the few similar-sized birds and lack tubercles).

Description and comparisons. The basihyal of the hyoid apparatus is narrow and rod-shaped (Figure 8M; note that the ossicle labelled as the basihyal of *Anachronornis* in Houde et al. 2023: figure 1Q is actually the paraglossum; the basihyal has a similar shape to that of *Danielsavis* [P. Houde, pers. comm. in review]). The ceratobranchials are not preserved in their complete length.

NMS.Z.2021.40.7 includes 15 presacral vertebrae, which, as far as comparisons are possible, correspond to the vertebrae of *Perplexicervix microcephalon* in their proportions. The atlas (Figure 8A, B) has a wide and dorsally open incisura fossae; unlike in *Danielsavis nazensis* it lacks foramina transversaria. Most unusually the dorsal portion of the arcus is absent, which appears to be a true – and almost certainly pathological – feature of the bone and not due to breakage, because the symmetrical dorsal ends of the arcus do not show the interior of the bone and are solid, with smooth surfaces. The axis (Figure 8C–E) is proportionally shorter than that of *D. nazensis* and the zygapophyses caudales are separated by a well-developed lacuna interzygapophysialis (in *Danielsavis* the caudal margin of the axis is straight); the dens is proportionally longer than in *Danielsavis*, the processus ventralis is broken. The vertebra we identify as the third cervical (Figure 8G, H) is also proportionally shorter and wider than the corresponding vertebra of *D. nazensis*. As in the latter species, it lacks an osseous bridge from the processus transversus to the zygapophysis (processus articularis) caudalis, but unlike in *D. nazensis* the cranial portion of the corpus vertebrae forms platform-like lateral sheets; the lacuna interzygapophysialis is shallow and the zygapophyses caudales bear cranially directed projections. The third vertebra, as well as the axis and another cervical, exhibit tuber-
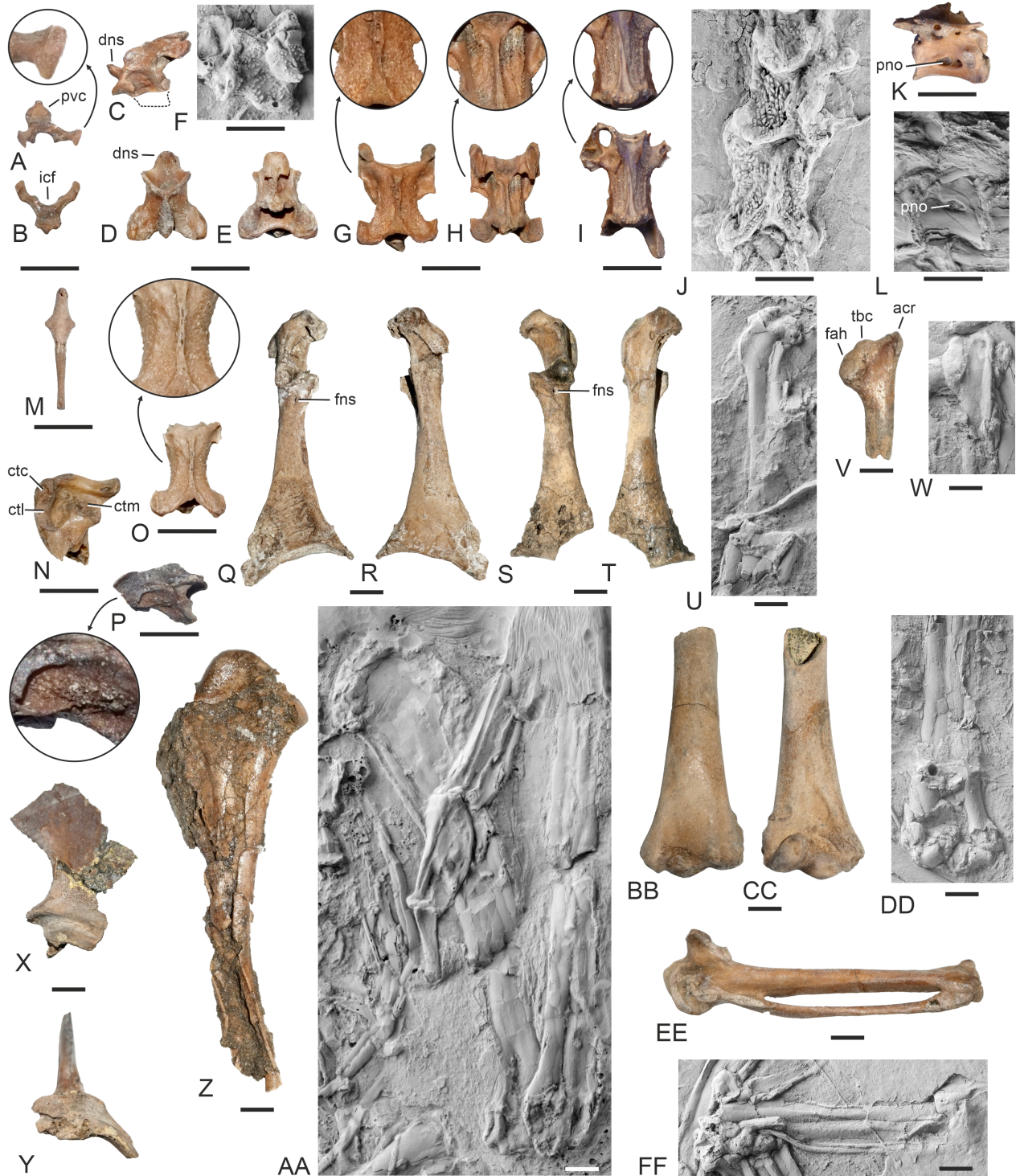
FIGURE 8 (caption on next page).

culate surfaces, which are densely covered with small "barb-like" processes (Figure 8G–I). In the holotype of *P. paucituberculata* the covering of the cervical vertebrae with barbs/tubercles is less extensive than in *P. microcephalon* from Messel, which is especially evident in the axis (Figure 8C, F). As in *P. microcephalon* (Figure 8L), the five thoracic vertebrae preserved in the holotype bear large pneumatic openings on their lateral surfaces (Figure 8K). One of the caudal vertebrae has club-

FIGURE 8 (figure on previous page). Selected skeletal elements of *Perplexicervix paucituberculata*, sp. nov. from the early Eocene London Clay of Walton-on-the-Naze (Essex, UK) and *P. microcephalon* from the latest early or earliest middle Eocene of Messel (Germany). **A, B,** atlas of *P. paucituberculata*, sp. nov. (holotype, NMS.Z.2021.40.7) in dorsal (**A**) and cranial (**B**) view; the arrow denotes a detail of the incomplete arcus atlantis. **C–E,** axis of *P. paucituberculata*, sp. nov. (holotype, NMS.Z.2021.40.7) in left lateral (**C**), dorsal (**D**), and ventral (**E**) view; the dotted line indicates the reconstructed shape of the broken processus ventralis. **F,** axis (lateral view) of *P. microcephalon* (SMF-ME 3548); coated with ammonium chloride. **G, H,** third cervical vertebra of *P. paucituberculata*, sp. nov. (holotype, NMS.Z.2021.40.7) in dorsal (**G**) and ventral (**H**) view; the arrows denote details of the tuberculate surface. **I,** cervical vertebra of *P. paucituberculata*, sp. nov. (holotype, NMS.Z.2021.40.7) in ventral view; the arrow denotes a detail of the tuberculate surface. **J,** fourth and fifth cervical vertebrae of *P. microcephalon* (holotype, SMF-ME 11211a); coated with ammonium chloride. **K,** thoracic vertebra of *P. paucituberculata*, sp. nov. (holotype, NMS.Z.2021.40.7). **L,** thoracic vertebra of *P. microcephalon* (SMF-ME 2559a); coated with ammonium chloride. **M,** os basiurohyale of *P. paucituberculata*, sp. nov. (holotype, NMS.Z.2021.40.7). **N,** caudal end of right mandibular ramus of *Perplexicervix* sp. (NMS.Z.2021.40.9) in dorsal view. **O,** cervical vertebra of *Perplexicervix* sp. (holotype, NMS.Z.2021.40.7); the arrow denotes a detail of the tuberculate surface. **P,** *Perplexicervix* sp., third cervical vertebra in lateral view (NMS.Z.2021.40.10); the arrow denotes a detail of the tuberculate surface. **Q, R,** left coracoid of *P. paucituberculata*, sp. nov. (NMS.Z.2021.40.91) in dorsal (**Q**) and ventral (**R**) view. **S, T,** right coracoid of *P. paucituberculata*, sp. nov. (NMS.Z.2021.40.92) in dorsal (**S**) and ventral (**T**) view. **U,** extremitas omalis of right coracoid of *P. microcephalon* (HLMD-Me 14996a) in ventral view; coated with ammonium chloride. **V,** extremitas cranialis of left scapula of *P. paucituberculata*, sp. nov. (NMS.Z.2021.40.92) in lateral view. **W,** extremitas cranialis of left scapula of *P. microcephalon* (HLMD-Me 14996b) in lateral view; coated with ammonium chloride. **X, Y,** cranial portion of sternum of *P. paucituberculata*, sp. nov. (NMS.Z.2021.40.92) in lateral (**X**) and cranial (**Y**) view. **Z,** proximal portion of right humerus of *P. paucituberculata*, sp. nov. (NMS.Z.2021.40.91) in cranial view. **AA,** left wing of *P. microcephalon* (HLMD-Me 14996a); coated with ammonium chloride. **BB, CC,** distal end of right humerus of *P. paucituberculata*, sp. nov. (NMS.Z.2021.40.92) in caudal (**BB**) and cranial (**CC**) view. **DD,** distal end of right humerus of *P. microcephalon* (HLMD-Me 14996b) in cranial view; coated with ammonium chloride. **EE,** left carpometacarpus of *P. paucituberculata*, sp. nov. (NMS.Z.2021.40.92) in ventral view. **FF,** right carpometacarpus of *P. microcephalon* (SMF-ME 11211b) in dorsal view; coated with ammonium chloride. **Abbreviations:** acr, acromion; ctc, cotyla caudalis; ctl, cotyla lateralis; ctm, cotyla medialis; dns, dens; fah, facies articularis humeralis; fns, foramen nervi supracoracoidei; icf, incisura fossae; pno, pneumatic opening; pvc, processus ventralis corporis; tbc, tuberculum coracoideum. The scale bars equal 5 mm.

shaped processus transversi with widened lateral ends and a bifurcate processus ventralis. The pygostyle is longer than the longest cervical vertebra, whereas it is shorter than the longest cervical in *Danielsavis*.

The coracoid of the tentatively referred specimens (Figure 8Q–T) is very unlike that of *Danielsavis*. The cotyla scapularis is deeply concave. The moderately long processus procoracoideus is broad in the sterno-omal direction. The facies articularis humeralis has a concave surface. A foramen nervi supracoracoidei is present but small and located close to the cotyla scapularis. The sternal margin of the bone is concave, the angulus medialis sharply pointed, and the processus lateralis fairly long. Compared to extant birds, the coracoid most closely resembles that of the Otidiformes (Figure 9B), with this similarity having already been noted by Mayr (2010) for *P. microcephalon.*

The scapula of the tentatively referred specimens (Figure 8V) has a short acromion and a pronounced tuberculum coracoideum. The facies articularis humeralis is more strongly ventrally protruding than in *P. microcephalon* (Figure 8W). The furcula bears a short apophysis furculae.

Only the cranial portion of the sternum is preserved (Figure 8X, Y), which bears a short spina externa. The carina sterni has a markedly concave cranial margin.

The humerus of the tentatively referred specimens is a fairly long and robust bone (Figure 8Z, BB, CC) and corresponds well to the humerus of *P. microcephalon* (Figure 8AA, DD) in the features that can be compared in the specimens. The caput humeri protrudes proximally, and the proximal end of the bone does not project much ventrally; the crista bicipitalis is poorly developed. On the distal end of the bone, the fossa musculi brachialis is fairly extensive, the condylus dorsalis is mediolaterally narrow, and the condylus ventralis forms the distalmost tip of the bone. As in *P. microcephalon*, the distoventral portion of the humerus is poorly developed and a processus flexorius not developed. The sulcus scapulotricipitalis is very shallow.

Only the proximal and distal ends of the ulna are preserved in the tentatively referred specimens (Figure 7B, C). As in *Danielsavis*, the cotyla dorsalis reaches much farther distally than the cotyla ventralis.
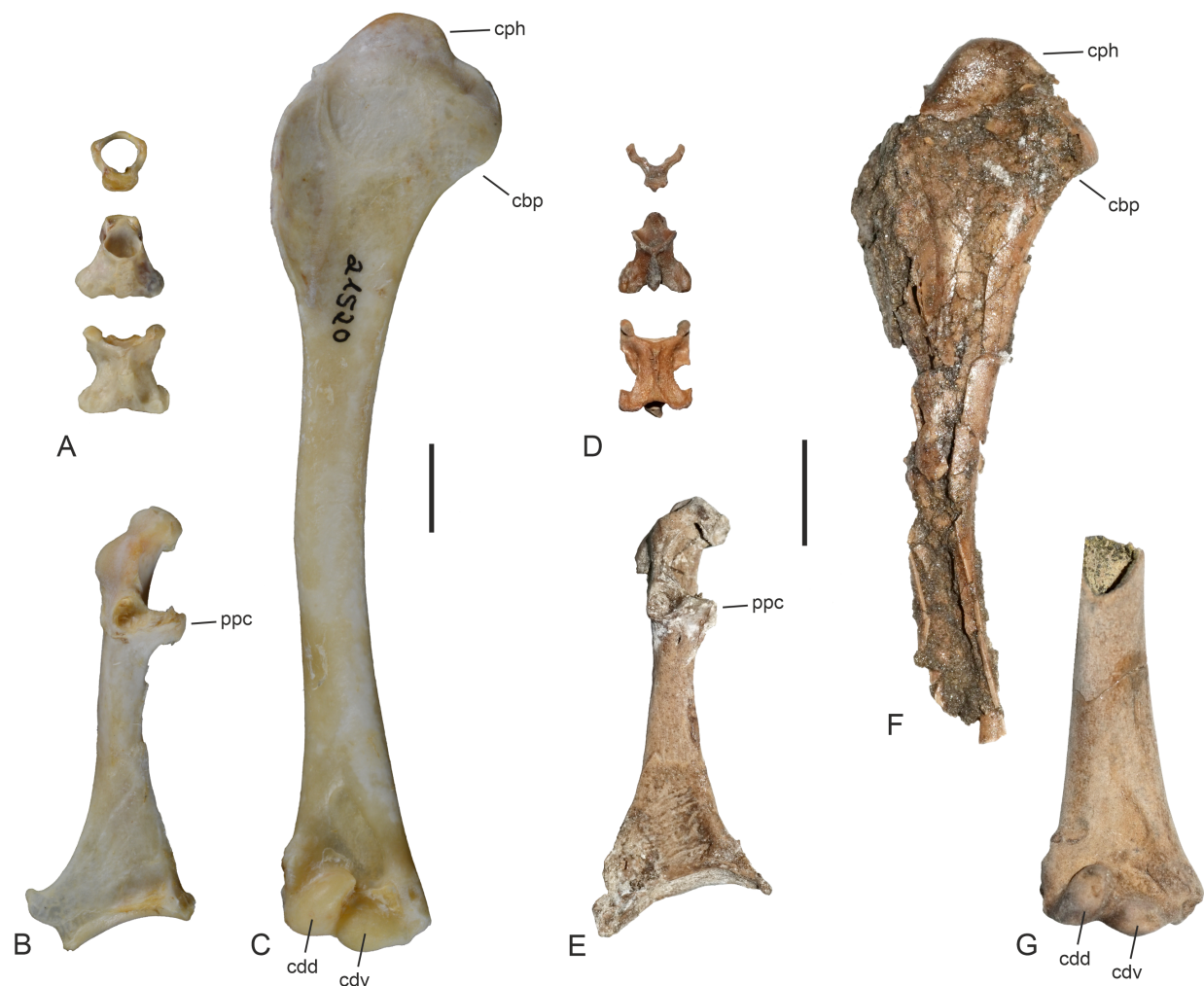
FIGURE 9. Comparison of selected skeletal elements of *Perplexicervix paucituberculata*, sp. nov. and *Eupodotis senegalensis* (Otidiformes) to illustrate similar proportions and morphologies. **A–C,** *E. senegalensis* (SMF 21520), first three cervical vertebrae (**A**), left coracoid (**B**), and right humerus (**C**). **D–G,** *P. paucituberculata*, sp. nov., first three cervical vertebrae (**D**), left coracoid (**E**), and proximal and distal ends of right humerus (**F, G**) (**D**: holotype, NMS.Z.2021.40.7; **E, F:** tentatively referred specimen NMS.Z.2021.40.91; **G:** tentatively referred specimen NMS.Z.2021.40.92). **Abbreviations:** cbp, crista bicipitalis; cdd, condylus dorsalis; cdv, condylus ventralis; cph, caput humeri; ppc, processus procoracoideus. The scale bars equal 10 mm.

The carpometacarpus of the tentatively referred specimen NMS.Z.2021.40.92 is long and narrow and has a long symphysis metacarpalis proximalis (Figure 8EE). The os carpi ulnare shows a rather unspecific morphology, with a moderately long crus longum. The os carpi radiale also resembles the radial carpal bone of various only distantly related birds, such as the Anatidae, Scolopacidae, and Phoenicopteridae (Mayr, 2014).

Perplexicervix sp.

Referred specimens. NMS.Z.2021.40.9 (Figure 7D; caudal portion of right mandibular ramus, fourth or fifth cervical vertebra, pygostyle). NMS.Z.2021.40.10 (Figure 7E; third cervical vertebra).

Remarks. The caudal portion of the mandible of NMS.Z.2021.40.9 (Figure 8N) exhibits a morphology characteristic of neoavian birds and is very different from the caudal mandible of *Danielsavis* and other galloanserines, in which there are two shallow cotylae that are separated by a longitudinal ridge running in parallel to the main axis of the mandible. The cotyla caudalis of *Perplexicervix* is pronounced, whereas it is absent in galloanserine birds, whose quadrates lack a condylus caudalis.
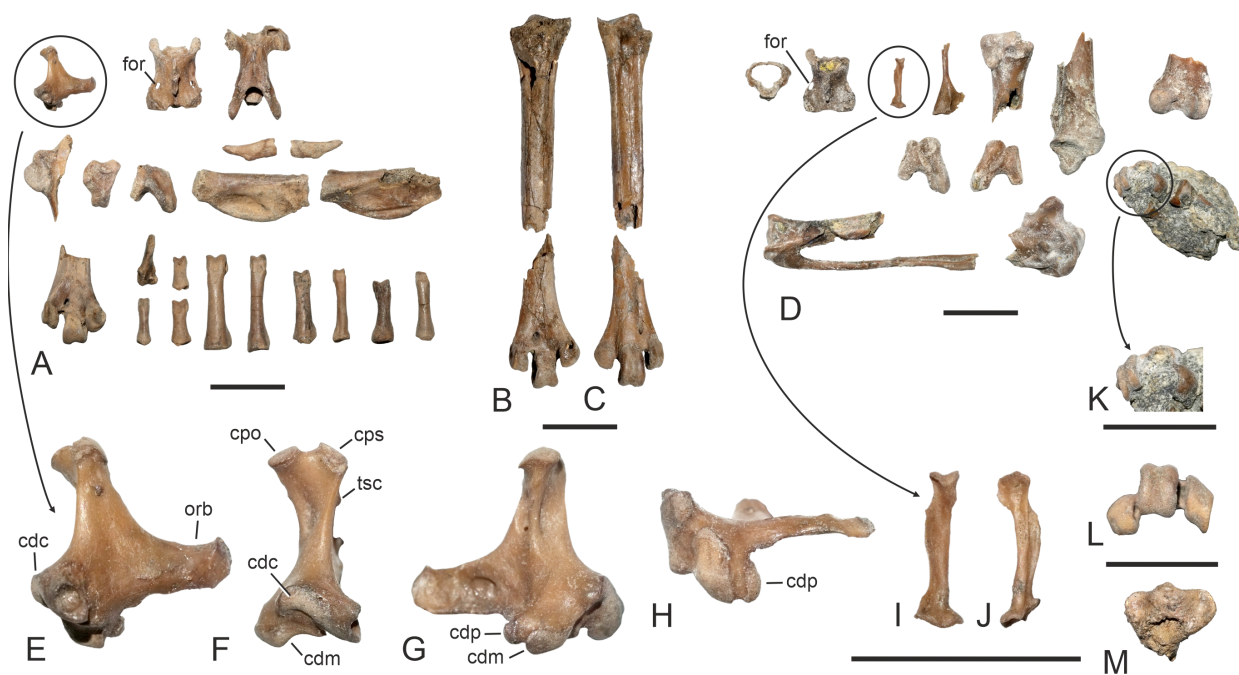
FIGURE 10. Undetermined birds that were likened to *Danielsavis* by Houde et al. (2023). **A,** partial skeleton of Aves indet. A (NMS.Z.2021.40.5). **B, C,** left tarsometatarsus of Aves indet. A (NMS.Z.2021.40.8) in plantar (**B**) and dorsal (**C**) view. **D,** partial skeleton of Aves indet. B (NMS.Z.2021.40.4). **E–H,** right quadrate of Aves indet. A (NMS.Z.2021.40.5) in lateral (**E**), caudal (**F**), medial (**G**), and ventral (**H**) view. **I, J,** right pterygoid of Aves indet. B (NMS.Z.2021.40.4) in lateral (**I**) and dorsal (**J**) view. **K,** distal end of right tarsometatarsus of Aves indet. B (NMS.Z.2021.40.4) in distal view. **L,** distal end of left tarsometatarsus of Aves indet. A (NMS.Z.2021.40.8) in distal view. **M,** proximal end of left tarsometatarsus of Aves indet. A (NMS.Z.2021.40.8) in proximal view. **Abbreviations:** cdc, condylus caudalis; cdm, condylus medialis; cdp, condylus pterygoideus; cpo, capitulum oticum; cps, capitulum squamosum; for, foramen; orb, processus orbitalis; tsc, tuberculum subcapitulare. The scale bars equal 10 mm.

In further contrast to *Danielsavis* and other Galloanseres, the mandible lacks a retroarticular process.

The two cervical vertebrae preserved in the specimens have a tuberculate surface (Figure 8O, P), but are smaller than the cervicals of the *P. paucituberculata* holotype (Figure 7A, D, E). The pygostyle of NMS.Z.2021.40.9 (Figure 7D) differs from that of the *P. paucituberculata* holotype in that the caudoventral portion of the corpus is perforated by a foramen.

Aves indet. A

Referred specimens. NMS.Z.2021.40.5 (Figure 10A; partial skeleton including right quadrate, two cervical vertebrae, cranial portion of left scapula, carpal bones and wing phalanges, distal end of left tarsometatarsus, pedal phalanges). NMS.Z.2021.40.8 (Figure 10B, C; partial left tarsometatarsus, pedal phalanges; the specimen was erroneously labeled as NMS.Z.2021.40.4 by Houde et al., 2023: figure 6E based on a misla-

beled image provided by M. Daniels [P. Houde, pers. comm. in review]).

Remarks. These two specimens were assigned to "group B" by Houde et al. (2023) and represent a species that was smaller than *Perplexicervix paucituberculata.* Houde et al. (2023) noted that the quadrate associated with NMS.Z.2021.40.5 (Figure 10E–H) exhibits three condyles, which precludes its assignment to the Galloanseres. The authors hypothesised that the bone may have been erroneously associated with the specimen, but in size it corresponds well to the other bones and there exists no indication that it was misplaced (even though we cannot conclusively exclude this possibility).

Unlike in *Danielsavis nazensis* and *P. paucituberculata*, the third cervical vertebra has an osseous bridge from the processus transversus to the zygapophysis caudalis, which delimits a small lateral foramen. The surfaces of the two cervical vertebrae preserved in NMS.Z.2021.40.5 lack tubercles. The acromion of the scapula is proportionally longer than in *Perplexicervix*. The tar-

17

sometatarsus is longer than that of *Danielsavis*. The hypotarsus is damaged, but does not seem to exhibit canals or sulci (Figure 10M). Unlike in *Danielsavis*, the plantar articulation surface of the trochlea metatarsi III is not asymmetric.

Aves indet. B

Referred specimen. NMS.Z.2021.40.4 (Figure 10D; partial skeleton including pterygoid, atlas and cervical vertebra, proximal and distal ends of right ulna, proximal and distal ends of right carpometacarpus, both ulnar carpal bones, distal end of right femur, distal end of right tarsometatarsus in a piece of matrix, pedal phalanges).

Remarks. This fossil was also assigned to "group B" by Houde et al. (2023), but is distinctly smaller than the specimens we refer to Aves indet. A (Figure 10 K, L). The pterygoid (Figure 10I, J) lacks a facies articularis basipterygoidea, which shows the fossil to be outside Galloanseres and also precludes possible affinities to *Perplexicervix* (because the skull of *P. microcephalon* from Messel does have basipterygoid processes). As in Aves indet. A, but unlike in *P. paucituberculata*, the third cervical vertebra exhibits an osseous bridge from the processus transversus to the zygapophysis caudalis, which delimits a small lateral foramen.

DISCUSSION

The Affinities of *Danielsavis*

The few analyses of Houde et al. (2023: figure S8) that included *Danielsavis* did not support anseriform affinities of the taxon. Instead, *Anachronornis* and *Danielsavis* resulted as successive sister taxa of crown group Galloanseres, with *Anachronornis* diverging before *Danielsavis* (Houde et al., 2023: figure 8C). Whereas *Anachronornis* was subjected to further analyses, which supported anseriform affinities, *Danielsavis* was not. Houde et al. (2023) nevertheless assigned *Danielsavis* to the Anseriformes, noting that the taxon is "[i]dentified as Anseriformes and distinguished from Galliformes (…) on the basis of the coracoid with large procoracoid process, foramen of the supracoracoid nerve, broad sternal extremity with flared lateral angle and absence of pneumatic foramen, and sternum without separate intermediate (…) and lateral (…) trabeculae" (Houde et al., 2023: 26). However, although these characters distinguish *Danielsavis* from galliforms, they may well be plesiomorphic for Galloanseres as a whole, and none represents an unambiguous anseriform apomorphy. For example, a foramen nervi supracoracoidei is present in the palaeognathous

Lithornithiformes (Houde, 1988) and the non-neornithine Ichthyornithidae (Clarke, 2004), and is likely to be plesiomorphic for neognathous birds.

Many of the diagnostic apomorphies of galliform birds are due to their pronounced capability of burst flights, which entailed a strongly developed supracoracoideus muscle and associated skeletal correlates. The galliform stem species may have been more "anseriform-like" in its postcranial skeleton, especially in characteristics of the pectoral girdle and wings, and it is not straightforward to determine whether *Danielsavis* is a galliform-like stem group anseriform or an anseriform-like stem group galliform. Even though the fossils were considered superficially "screamer-like" by Mayr (2022) and Houde (2023), *Danielsavis* is clearly outside crown group Anseriformes. Plesiomorphic features in which the fossil taxon differs from all extant anseriforms include: (1) a mandible with dorsoventrally very low rami; (2) palatine bones without co-ossified caudal portions; (3) a quadrate with a foramen pneumaticum basiorbitale (this foramen is absent or vestigial in crown group Anseriformes; Elzanowski and Stidham, 2010); (4) a palatine bone without a distinct angulus caudolateralis; (5) a much smaller paraglossum (if our identification of this ossicle in the *D. nazensis* holotype is correct); (6) a carpometacarpus without a proximocaudally projected trochlea carpalis; (7) a tibiotarsus with a medially situated sulcus extensorius (in anseriforms this sulcus is centrally located); and (8) proportionally shorter phalanges of the fourth toe.

Compared to *Danielsavis*, *Anachronornis* is much more anseriform-like in that the upper beak has a broadly rounded tip, the lower jaw has proportionally deeper rami mandibularum, the humerus is more elongated and with a smaller proximal end, the carpometacarpus has a proximocaudally projected trochlea carpalis, the trochlea metatarsi II is proportionally shorter, and the pedal phalanges are proportionally longer. The dorsoventrally low mandibular rami support a position of *Danielsavis* outside a clade including *Anachronornis, Conflicto,* presbyornithids, and crown group Anseriformes. Of *Nettapterornis*, which co-existed with *Danielsavis* in the paleoenvironment of Walton-on-the-Naze, only the caudal end of the mandible is known (Olson, 1999), but the taxon is obviously more anseriform-like than *Danielsavis* in its spatulate and very "duck-like" beak (Olson, 1999); the holotype of *Nettapterornis oxfordi* lacks hindlimb elements, but the Daniels collection includes a tarsometatarsus of a juvenile anseriform

bird (Mayr, 2022: figure 4.12b), which – judging from its similar large size – most likely stems from *N. oxfordi* and is also much more anseriform-like than the tarsometatarsus of *Danielsavis*. The lengths of the pedal phalanges are unknown for *Nettapterornis* and *Conflicto*, but *Anachronornis* and *Presbyornis* have elongated phalanges similar to those of crown group Anseriformes (Musser and Clarke, 2022: figure 4H; Houde et al., 2023: table S1). The coracoids of *Anachronornis, Conflicto, Nettapterornis,* and presbyornithids bear a proportionally larger processus acrocoracoideus than the coracoid of *Danielsavis* and the humeri are slenderer (Figure 5). Therefore, if *Danielsavis* is a stem group anseriform, it is likely to be the basalmost one currently known and is more distantly related to crown group Anseriformes than is *Anachronornis* (*contra* Houde et al., 2023).

Danielsavis exhibits the following characteristics of anseriform birds, most of which show homoplasy within Galloanseres or Neornithes: (1) a pterygoid with a strongly protruding facies articularis basipterygoidei (the pterygoid of *Danielsavis* closely resembles that of *Nettapterornis*, but a similar pterygoid morphology is also found in the Gastornithidae [Mayr, 2022: figure 4.5b] and may be plesiomorphic for Galloanseres); (2) a flange-like process for the attachment of musculus adductor mandibulae externus on the lateral surface of the mandible (this process is absent in the anseriform Anhimidae and present in the galliform Megapodiidae); (3) an atlas that exhibits foramina transversaria (these foramina are absent in *Anachronornis* and the Anhimidae); (4) thoracic vertebrae with pneumatic openings (these openings occur in the palaeognathous Lithornithidae and may be plesiomorphic for neornithine birds, with their absence in the Galliformes possibly being due to the fact that the thoracic vertebrae of galliforms are co-ossified to form a notarium; Mayr, 2021); and (5) a furcula with long processus acromiales (long acromial processes are also present in the palaeognathous Lithornithidae and may be plesiomorphic for neornithine birds).

Some hindlimb features in which *Danielsavis* agrees with galliforms are likely to be plesiomorphic, such as the medially situated sulcus extensorius of the tibiotarsus (a medial sulcus occurs in the palaeognathous Lithornithiformes and Tinamiformes and in most non-anseriform neognathous birds), the short toes, and possibly also the asymmetric plantar articular surface of the trochlea metatarsi III, in which the lateral rim reaches farther proximally than the medial one (Mayr, 2000 considered this morphology to be an apomorphy of Galliformes, but in a somewhat less pronounced form it is also present in *Anachronornis* [Figure 6N] and may therefore be plesiomorphic for Galloanseres; in crown group Anseriformes the articular surface of the trochlea metatarsi III is elongated and of subtriangular shape).

Other features shared by *Danielsavis* and galliform birds concern the pectoral girdle and wing bones, and are less easily explained as plesiomorphic resemblances. This is especially true for the coracoid (Figure 5A, B), which, except for the long processus procoracoideus and the presence of a crista procoracoidei and foramen nervi supracoracoidei, is more similar to that of early Eocene stem group galliforms (Figure 5C) than to the coracoid of unambiguous anseriforms (Figure 5D–F). In particular, the coracoid of *Danielsavis* resembles that of early Eocene stem group Galliformes in the shape of the omal extremity, which is proportionally shorter than in most anseriforms and has a smaller processus acrocoracoideus. Outgroup comparisons with the palaeognathous Lithornithiformes suggest that the proportions of the omal extremity of anseriforms, rather than those of galliforms, are plesiomorphic for galloanserine birds, and this is particularly likely under the assumption that the burst-flight capability of galliforms is a derived characteristic of these birds. The proximal end of the ulna of *Danielsavis* likewise differs from that of anseriforms and corresponds to that of galliform birds concerning the long cotyla dorsalis (Figure 5R–T). Outgroup comparisons with the Ichthyornithidae and Lithornithidae again suggest that the long cotyla dorsalis is a derived characteristic. *Danielsavis* also has a stouter humerus than unambiguous anseriforms (Figure 5L–Q) and the tuberculum dorsale is proportionally longer, even though it does not reach the size of this tubercle in galliform birds, in which the tuberculum dorsale forms a long attachment scar for the supracoracoideus muscle (Figure 5P).

Our analysis of the emended dataset 1 of Houde et al. (2023), the only one including *Danielsavis*, resulted in three most parsimonious trees. In the strict consensus tree (Figure 11A), *Danielsavis*, *Anachronornis*, crown group Anseriformes, and the galliform taxon *Crax* are placed in a polytomy. By contrast, the majority rule consensus tree (Figure 11B) shows *Danielsavis* and *Crax* to be sister taxa (this topology was found in two of the resulting trees, whereas the third tree recovered *Anachronornis* and *Danielsavis* as successive sister taxa of crown group Galloanseres). Our analysis of this
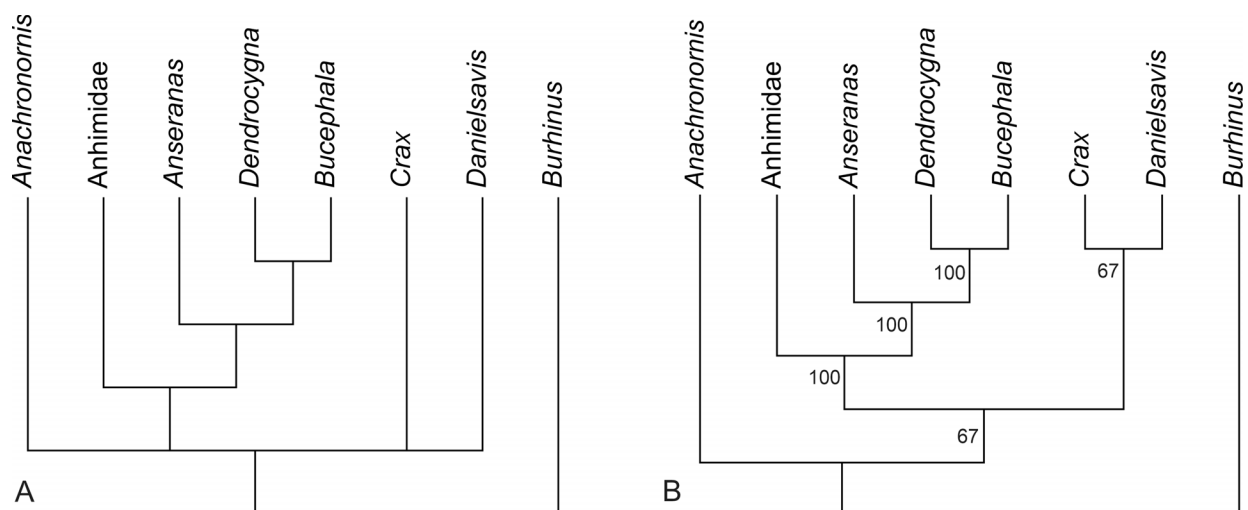
FIGURE 11. Results of the analysis of the emended dataset 1 of Houde et al. (2023). **A,** strict consensus tree of three most parsimonious trees (length = 317, consistency index = 0.69, retention index = 0.50). **B,** majority rule consensus tree with values indicating the percentage of trees in which the respective node is retained.

dataset agreed with the analyses of Houde et al. (2023) in that it did not support anseriform affinities of *Anachronornis*. By contrast, Houde et al.'s (2023) analyses of other datasets (which did not include *Danielsavis*) recovered *Anachronornis* as an anseriform, which is supported by, e.g., the broadly rounded tip of the beak of the taxon and the shape of the rostrally directed processus postorbitalis.

Clearly, the affinities of *Danielsavis* still have to be analysed in a broader taxonomic context before well-founded conclusions can be drawn. However, anseriform affinities of the taxon are only weakly supported, and even though *Danielsavis* exhibits some anseriform characteristics, most of these show homoplasy within Galloanseres. The galliform-like features of the pectoral girdle and wing bones likewise do not represent strong evidence for an identification of *Danielsavis* as an archaic stem group galliform, but this possibility needs to be considered in future studies.

The Affinities of *Perplexicervix*

Some of the fossils that are here referred to *Perplexicervix* were assigned to "group C" by Houde et al. (2023), who did not directly examine these specimens and appear to have based their assignment to the Anseriformes on the fact that Mayr (2010, 2022) likened *Perplexicervix* to the Anhimidae. However, even though *P. microcephalon* and extant Anhimidae share basipterygoid processes and large pneumatic openings on the lateral surfaces of the thoracic vertebrae, the mandible of specimen NMS.Z.2021.40.9 from Walton-on-the-Naze exhibits a neoavian morphology, which conflicts with galloanserine affinities of *Perplexicervix*.

The coracoid of the tentatively referred specimen shows a strong resemblance to that of the Otidiformes (bustards; Figure 9B, E), which especially applies to the shape of the extremitas omalis with its deeply excavated cotyla scapularis and broad processus procoracoideus. The humerus likewise resembles that of otidiforms in the morphologies of the proximal and distal ends, in particular with regard to the proximally protruding caput humeri, the weakly developed crista bicipitalis, and the configuration of the distal condyles (Figure 9C, F, G). The vertebrae also correspond to those of otidiforms in their morphology (Figure 9A, D), but these similarities are rather unspecific, and in extant bustards the central cervicals are more elongated. The thoracic vertebrae of extant Otidiformes lack large pneumatic foramina but exhibit irregularly distributed small openings in their lateral surfaces (Mayr, 2021). The Otidiformes have no published Paleogene fossil record (Mayr, 2022), and recognition of perplexicervicids as early stem group representatives would close a significant gap in the fossil record of these Old World birds. However, our tentative assignment of the fossils to the Otidiformes is merely based on an overall similarity of the major limb bones preserved in the fossils to those of the Otidiformes, and unambiguous character evidence for a phylogenetic placement of *Perplexicervix* has yet to be identified. Unlike in extant Otidiformes, the skull of *P. microcephalon* exhibits basipterygoid processes (Mayr, 2007,

2010). These processes are also present in the Musophagiformes, which in current sequence-based analyses result as the sister taxon of either the Otidiformes (Kuhl et al., 2021) or a clade including the Otidiformes and Cuculiformes (Prum et al., 2015), and basipterygoid processes may therefore be plesiomorphic for otidiforms.

An isolated vertebra with a tuberculate surface is also known from a late Eocene deposit of the Quercy fissure fillings in France (Mayr, 2007). This specimen is of interest, because Mourer-Chauviré (2006) mentioned unpublished remains of putative Otidiformes from an unknown stratigraphic horizon of the Quercy fissure fillings. Given the resemblance of the postcranial bones we refer to *Perplexicervix* to the corresponding skeletal elements of the Otidiformes, it is possible that the vertebra and the undescribed otidiform-like fossils from the Quercy fissure fillings belong to the same taxon. If so, these fossils are likely to stem from a member of the Perplexicervicidae and may provide further insights into the affinities of this taxon.

The fact that the atlas of the *P. paucituberculata* holotype appears to show a pathological morphology may support the hypothesis that the vertebral tubercles are likewise of pathological origin (Mayr, 2007, 2010). However, the presence of tuberculate vertebrae in multiple individuals speaks against this assumption, and we therefore consider the tubercles to be a true morphological feature and to represent a diagnostic apomorphy of the Perplexicervicidae. The functional significance of these structures remains unknown.

Tuberculate vertebrae are unknown from extant birds, but occur in a large avian species from Messel, which was described as *Idiornis* (= *Dynamopterus) tuberculata* by Peters (1995), who assigned the fossil to the cariamiform Idiornithidae. The poor preservation of the holotype allows the examination of only a few morphological details, but apart from its much larger size, and as far as comparisons are possible, *"I." tuberculata* mainly differs from the species of *Perplexicervix* in features related to its proportionally much shorter wings. If the tuberculate vertebrae are autapomorphic for the Perplexicervicidae, *"I." tuberculata* may possibly be a large flightless member of the new taxon.

ACKNOWLEDGEMENTS

REFERENCES

Aldiss, D.T. 2012. The stratigraphical framework for the Palaeogene successions of the London Basin, UK. British Geological Survey Open Report, OR/12/004:1–87.

Clarke, J.A. 2004. Morphology, phylogenetic taxonomy, and systematics of *Ichthyornis* and *Apatornis* (Avialae: Ornithurae). Bulletin of the American Museum of Natural History, 286:1–179.
https://doi.org/10.1206/0003-0090(2004)286<0001:MPTASO>2.0.CO;2

Collinson, M.E., Adams, N.F., Manchester, S.R., Stull, G.W., Herrera, F., Smith, S.Y., Andrew, M.J., Kenrick, P., and Sykes, D. 2016. X-ray micro-computed tomography (micro-CT) of pyrite-permineralized fruits and seeds from the London Clay Formation (Ypresian) conserved in silicone oil: a critical evaluation. Botany, 94:697–711.
https://doi.org/10.1139/cjb-2016-0078

De Pietri, V.L., Scofield, R.P., Zelenkov, N., Boles, W.E., and Worthy, T.H. 2016. The unexpected survival of an ancient lineage of anseriform birds into the Neogene of Australia: the youngest record of Presbyornithidae. Royal Society Open Science, 3:150635.
https://doi.org/10.1098/rsos.150635

Elzanowski, A. and Stidham, T.A. 2010. Morphology of the quadrate in the Eocene anseriform *Presbyornis* and extant galloanserine birds. Journal of Morphology, 271:305–323.
https://doi.org/10.1002/jmor.10799

Ericson, P.G.P. 2000. Systematic revision, skeletal anatomy, and paleoecology of the NewWorld early Tertiary Presbyornithidae (Aves: Anseriformes). PaleoBios, 20:1–23.

Field, D.J., Benito, J., Chen, A., Jagt, J.W., and Ksepka, D.T. 2020. Late Cretaceous neornithine from Europe illuminates the origins of crown birds. Nature, 579:397–401.
https://doi.org/10.1038/s41586-020-2096-0

Houde, P. 1988. Palaeognathous birds from the early Tertiary of the Northern Hemisphere. Publications of the Nuttall Ornithological Club, 22:1–148.

Houde, P., Dickson, M., and Camarena, D. 2023. Basal Anseriformes from the Early Paleogene of North America and Europe. Diversity, 15(2):233.
https://doi.org/10.3390/d15020233

Jolley, D.W. 1996. The earliest Eocene sediments of eastern England: an ultra-high resolution palynological correlation. In Knox, R.W.O'B., Corfield, R.M., and Dunay, R.E. (eds.), Correlation of the Early Paleogene in Northwest Europe. Geological Society of London, Special Publications, 101:219–254.
https://doi.org/10.1144/GSL.SP.1996.101.01.14

Kuhl, H., Frankl-Vilches, C., Bakker, A., Mayr, G., Nikolaus, G., Boerno, S.T., Klages, S., Timmermann, B., and Gahr, M. 2021. An unbiased molecular approach using 3'UTRs resolves the avian family-level tree of life. Molecular Biology and Evolution, 38:108–127.
https://doi.org/10.1093/molbev/msaa191

Kurochkin, E.N. and Dyke, G.J. 2010. A large collection of *Presbyornis* (Aves, Anseriformes, Presbyornithidae) from the late Paleocene and early Eocene of Mongolia. Geological Journal, 45:375–387.
https://doi.org/10.1002/gj.1177

Linnaeus, C. 1758. Systema naturae per regna tria naturae. 10th edition, 2 vols. L. Salmii, Holmiae.

Mayr, G. 2000. A new basal galliform bird from the Middle Eocene of Messel (Hessen, Germany). Senckenbergiana lethaea, 80:45–57.
https://doi.org/10.1007/BF03043663

Mayr, G. 2007. Bizarre tubercles on the vertebrae of Eocene fossil birds indicate an avian disease without modern counterpart. Naturwissenschaften, 94:681–685.
https://doi.org/10.1007/s00114-007-0241-3

Mayr, G. 2010. A new avian species with tubercle-bearing cervical vertebrae from the Middle Eocene of Messel (Germany). In Boles, W.E. and Worthy, T.H. (eds.), Proceedings of the VII International Meeting of the Society of Avian Paleontology and Evolution. Records of the Australian Museum, 62:21–28.
https://doi.org/10.3853/j.0067-1975.62.2010.1537

Mayr, G. 2014. Comparative morphology of the radial carpal bone of birds and the phylogenetic significance of character variation. Zoomorphology, 133:425–434.
https://doi.org/10.1007/s00435-014-0236-5

Mayr, G. 2021. On the occurrence of lateral openings and fossae (pleurocoels) in the thoracic vertebrae of neornithine birds and their functional significance. Vertebrate Zoology, 71:453–463.
https://doi.org/10.3897/vz.71.e71268

Mayr, G. 2022. Paleogene fossil birds, 2nd edition. Springer, Cham.
https://doi.org/10.1007/978-3-030-87645-6

Mourer-Chauviré, C. 2006. The avifauna of the Eocene and Oligocene Phosphorites du Quercy (France): an updated list. Strata, série 1, 13:135–149.

Musser, G. and Clarke, J.A. 2022. A new Paleogene fossil and a new dataset for waterfowl (Aves: Anseriformes) clarify phylogeny, ecological evolution, and avian evolution at the K-Pg Boundary. bioRxiv preprint.
https://doi.org/10.1101/2022.11.23.517648

Olson, S.L. 1999. The anseriform relationships of *Anatalavis* Olson and Parris (Anseranatidae), with a new species from the Lower Eocene London Clay. Smithsonian Contributions to Paleobiology, 89:231–243.

Olson, S.L. and Feduccia, A. 1980. *Presbyornis* and the origin of the Anseriformes (Aves: Charadriomorphae). Smithsonian Contributions to Zoology, 323:1–24.
https://doi.org/10.5479/si.00810282.323

Peters, D.S. 1995. *Idiornis tuberculata* n. spec., ein weiterer ungewöhnlicher Vogel aus der Grube Messel (Aves: Gruiformes: Cariamidae: Idiornithinae). Courier Forschungsinstitut Senckenberg, 181:107–119.

Prum, R.O., Berv, J.S., Dornburg, A., Field, D.J., Townsend, J.P., Lemmon, E.M., and Lemmon, A.R. 2015. A comprehensive phylogeny of birds (Aves) using targeted next-generation DNA sequencing. Nature, 526:569–573.
https://doi.org/10.1038/nature15697

Rayner, D., Mitchell, T., Rayner, M., and Clouter, F. 2009. London Clay fossils of Kent and Essex. Medway Fossil and Mineral Society, Rochester, Kent.

Sibley, C.G., Ahlquist, J.E., and Monroe Jr, B.L. 1988. A classification of the living birds of the world based on DNA-DNA hybridization studies. The Auk, 105:409–423.
https://doi.org/10.1093/auk/105.3.409

Swofford, D.L. 2002. PAUP* Phylogenetic analysis using parsimony (*and other methods), version 4.0b10. Sinauer Associates, Sunderland [computer software].

Tambussi, C.P., Degrange, F.J., De Mendoza, R.S., Sferco, E., and Santillana, S. 2019. A stem anseriform from the early Palaeocene of Antarctica provides new key evidence in the early evolution of waterfowl. Zoological Journal of the Linnean Society, 186:673–700.
https://doi.org/10.1093/zoolinnean/zly085

Zelenkov, N.V. 2021. A Revision of the Palaeocene–Eocene Mongolian Presbyornithidae (Aves: Anseriformes). Paleontological Journal, 55:323–330.
https://doi.org/10.1134/S0031030121030138

Zusi, R.L. and Livezey, B.C. 2006. Variation in the os palatinum and its structural relation to the palatum osseum of birds (Aves). Annals of Carnegie Museum, 75:137–180.
https://doi.org/10.2992/0097-4463(2006)75[137:VITOPA]2.0.CO;2